The Vibration of Plywood Plates by Experiment and Finite Element Analysis: Edge Constraints and Box Structures

John Coffey, Cheshire, UK.

December 2012, extended February 2013

Key words: orthotropic, birch plywood, glued edge, boundary conditions, violin, finite element, Strand7 and LISA 8 programs, resonant modes and frequencies, FEA compared to experiment.

1 Introduction

This article is the fourth in a series describing my personal studies into the acoustics of the violin and viola. Though this complex subject already has a large literature, I have been carrying out my own investigations to gain a first hand understanding. My earlier articles are published on www.mathstudio.co.uk, the one immediately preceding this being 'The orthotropic elastic constants and vibrational modes of plywood plates by experiment and finite element analysis'. It deals with free (unsupported) plates. This current article takes the study a step further by examining the effects of the boundary conditions where plates are fixed to other wooden sections to make a box structure such as the resonant belly of a violin-family musical instrument. I have investigated only natural modes, not the dynamic response to a prescribed driving force – that will be dealt with in a later paper.

In a violin the plates are glued to the ribs (thin curved side panels), traditionally with animal glue, the joint being reinforced all round on the inside by a fillet of wood with triangular section. This edge restraint affects the vibrational pattern and frequencies of the plate. In terms of mathematical modelling it is known that the solution of differential equations in general can be influenced strongly by the boundary conditions, which typically describe restrictions to the displacement, gradient, rotation, velocity, stress, etc. at the edges of the region being modelled. In any actual violin we cannot know precisely the restraints at every position around the rim of the top and bottom plates as these may depend on the thickness and age of the glue and wooden fillet, and whether knocks in the past have cracked the joint. In addition, the rim of a violin has 'purfling' which is a strip of wood inlaid into a groove positioned 3 or 4 mm inside the plate edge, roughly in line with the ribs. The purfling groove (Figure 1) is cut through about half the depth of the plate. Despite being filled with the purfling inlay, it is reported in the literature to increase the flexibility at the edge, making the joint closer to hinged rather than rigid.

This present study continues to use the Strand7 finite element program and compares its model predictions with experimental results on single glued plates. Towards the end of the study a pre-release copy of LISA 8 became available and this is compared with experiment on a closed plywood box in §4.2. The plates used throughout this paper have been flat so that Chladni figures could be obtained experimentally.

Figure 1: Cutting the purfling groove. (Picture from the internet)

2 Boundary constraints on a single rectangular plate

One challenge in the study has been to represent different realistic fixing conditions within the finite element model. Where 2D plate-shell elements represent a plate, at each node there are six values which can be fixed: free or fixed displacements in x, y, z and free or fixed rotation about the x, y or z axes. These are on-off conditions. In a 2D model flexible joints representing soft, pliable glue might be represented by ribs with jelly-like compliance. With a 3D model using brick elements is should be possible to represent pliable glue with flexible brick elements between adjacent wooden sections.

A small number of mathematically idealised plate edge conditions are well recognised. The term 'simply supported' applied to a beam means one resting under its own weight between two knife-edge supports. The transverse displacement u at the supports is zero, as is the bending moment so the second derivative u'' is also zero. There is no in-plane restraint force. However, the beam can tip at its supports so in general the gradient u' there is non-zero. The simply supported (SS) condition is sometimes modelled by having a hinged connection at one edge and a pair of rollers at the opposite, the rollers holding the plate without in-plane restraint whilst allowing hinged motion. A plate which is hinged at both opposite edges but with no displacement would experience in-plane pulling and pushing as the plate flexes.

A fixed (clamped) beam or plate edge cannot be displaced and cannot rotate, so both u and u' are zero. The edge will sustain bending moments so the plate will in general curve at the edge, corresponding to u'' being non-zero. A practical example would be a steel sheet welded around its edges into a heavy frame.

In a violin there is the somewhat different condition of a plate being glued to thin elastic ribs whose stiffness comes mainly from being curved. Restrain by the ribs will affect the vibration of top and bottom plates in addition to the restrain imposed by the glued joint. For this reason the model of violin plate vibration needs to be developed to represent a box structure with thin elastic sides.

In addition to the plate edge conditions, a violin has a sound post – an internal pencil-like rod of pine wood wedged between the top and back plates near the right foot of the bridge. The sound post is not glued, but held in place by friction under the clamping force of the taut strings. Modelling this would require non-linear point contact finite elements.

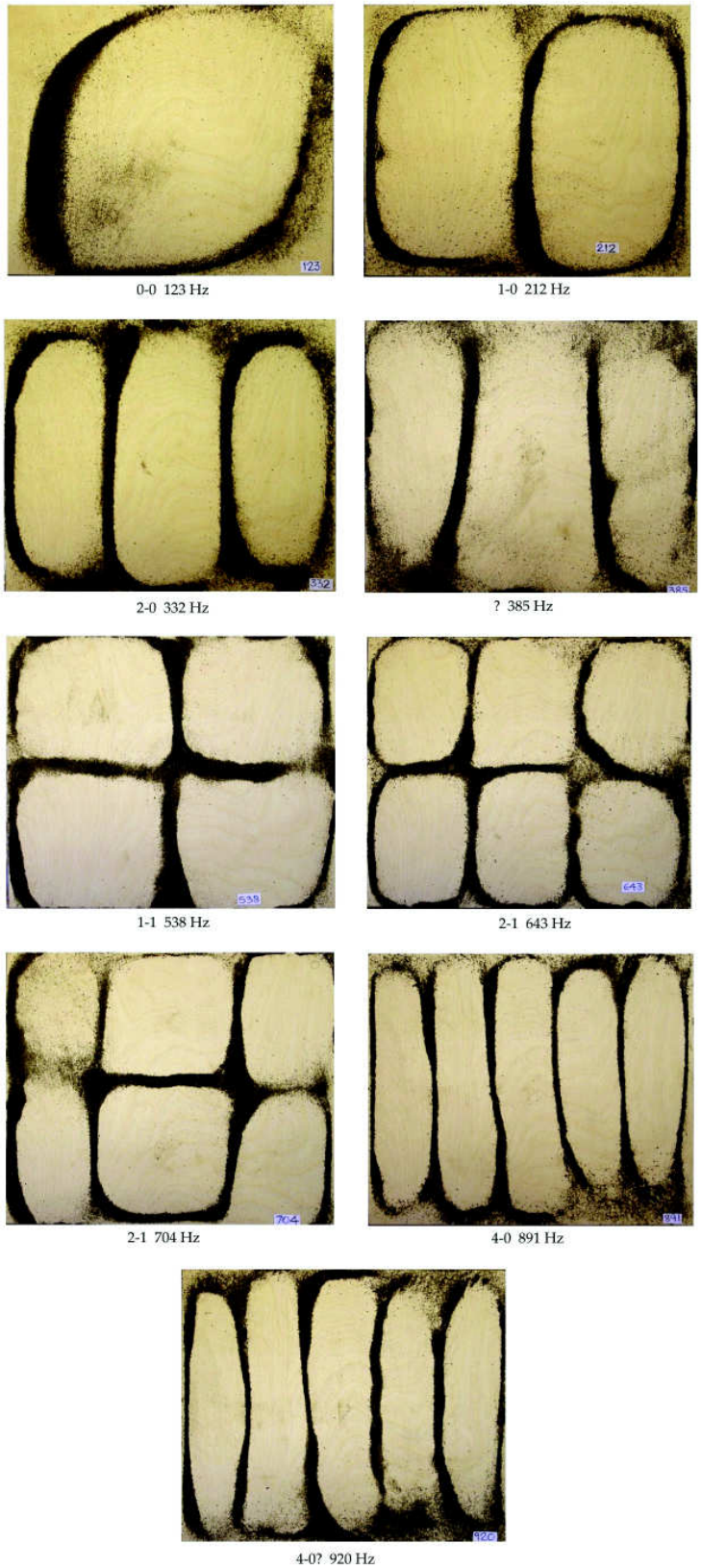

Figure 2: Chladni figures of an all-birch 3-ply plate 300mm across grain, 250mm along grain, $3 \cdot 65$ mm thick glued round all edges by hot melt adhesive to an MDF frame.

2.1 Experimental measurements on an edge-glued plated

Some experimental results will readily show the main effect of constraint around the plate edges. I used the 3·65 mm thick rectangular plate of all-birch 3-ply, 300 mm across the grain by 250 mm along the grain from the previous study. In that the modes of free vibration had been comprehensively measured – refer to Figures 2, 3 and 4 of the previous article on orthotropic elastic constants and vibrational modes. For this present study I glued the plate to a frame of 15 mm thick MDF. The plate overlapped the frame by 2 mm at each edge and the glue was a roughly triangular fillet across the right angle formed by plate edge and frame. I used hot melt adhesive from a hobby gun because it is flexible, rather rubbery, and would allow some small motion. It probably approximates a hinged SS joint. As previously, tap sounds were recorded and the peaks in the frequency spectra of about six taps noted. Then Chladni figures were obtained by exciting the plate with the electromagnetic acoustic exciter driven with a continuous signal at each of these prominent frequencies in turn. The only notable difference from the previous experimental technique was that the exciter was inverted and rested on the top surface of the plate, rather than the plate resting on the exciter.

Figure 2 shows a selection of modes. There is always a node around the edge where the glue prevents almost all motion except some rotation around the line of glue. This type of motion is simpler than that of a free plate in that the node lines divide the length and breadth of the plate into an integer number of equal sections. The displacement is described by a sinusoidal variation with position, with nodes at the edges. Thus the plate length is divided into an integral number of half cycles. The notation for the modes counts only the nodal lines inside the plate boundary, excluding the boundary itself.

I found these modes less easy to excite and less distinct in frequency and Chladni figure than with the free plate. This can be attributed in part to the constraint restricting motion, and partly to the leakage of energy into the glue and thence into the MFD frame.

2.2 Normal modes of 2D plate-shell element models

The first study with Strand7 has been to calculate the normal modes and frequencies of a single rectangular plate of all-birch 3-ply under nine boundary conditions. Some of these involve what I call a 'stitched edge' in which alternate lengths of the perimeter are assigned these different boundary conditions: i) free then simply supported (SS), ii) free then fixed, iii) simply supported then fixed. The stitching pattern is shown in Figure 3.

The nine conditions modelled, in rough order of increasing constraint, are

1. all four edges free,
2. stitched, alternately free (blue in Figure 3) and SS (pale yellow),
3. SS with purfling, represented by reduction of the notional plate element thickness to $1 \cdot 8$ mm over all elements one in from the edge,
4. plate supported on four ribs of highly compliant, glue-like material,
5. SS – all four edges hinged and with no out-of plane displacement but with in-plane displacement allowed,
6. all edges hinged but with no displacement in any direction,

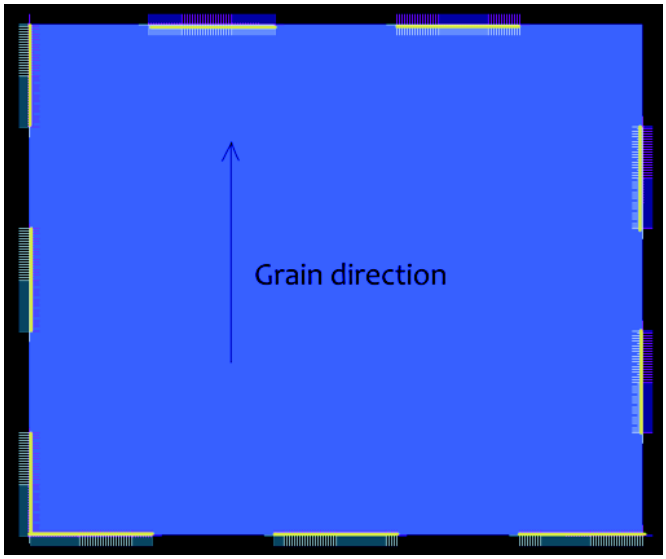

Figure 3: 'Stitched edge'. The rectangular plate modelling in Strand7 showing sections of edge in alternating pale yellow then blue at which different constraints have been applied.

7. 'stitched' with successive segments alternately free (blue in Figure 3) then fixed (pale yellow). This represents a glued joint which has come apart in places.

8. stitched with alternately SS (yellow) then fully fixed (blue). This represents a joint which is heavily over-glued in sections.

9. all edges fully clamped.

In the previous article the effective elastic constants had been determined. In GPa these are

$$E_1 = 17 \cdot 93, \quad E_2 = 2 \cdot 002, \quad G_{12} = 0 \cdot 781, \quad G_{23} = 0 \cdot 50, \quad G_{31} = 0 \cdot 242,$$

with $\nu_{12} \approx 0$. Table 16 of the previous article presents both the calculated and measured modal frequencies of this plate when all its edges are free. This is a reference for comparison with the various degrees of constrained motion.

Calculations under the above nine conditions were carried out using Strand7 FEA with the above elastic constants. The mesh had 12,000 square quad9 shell-plate elements each with side length 5 mm. The calculated resonant frequencies are listed in Table 1. The left and right hand columns notate the modes for the extreme conditions of constraint, free and fixed. There was negligible difference between cases 4 and 5; they both may be called SS. Figure 4 shows example contours of displacement, comparing the SS case (left column) with the stitched free+SS case (right) for nominally the same modes. The stitched case (right) shows little change in mode shape at low frequencies – there is negligible change for modes 1, 2 and 3 in the mode table – but by mode 13 (bottom pair in Figure 5) the free sections of edge have so allowed the plate to vibrate that the displacement contours are almost entirely different from the all-SS case.

The clear message of these results is that any form of constraint changes the nodal pattern and drives up the resonant frequencies strongly. Even a modest amount of constraint can have a large effect. The effect is largest for the lower modes. In particular the jumps in the lowest resonance, from 54 Hz for free to 144 Hz for simply supported to 306 Hz for clamped edges are remarkable –

nearly a 6-fold increase. There is a marked change in displacement pattern from free to constrained, but a smaller change in shape amongst the various type of constraint. To emphasise the effects of increasing constraint, Figure 5 plots the increase in frequency with mode number (in the table of modes listed in order of increasing frequency) for six of the constraint conditions.

Mode	fully free	50% free+SS	SS+ purfling	soft glue	SS	50% free+fixed	50% SS+fixed	fully fixed	Mode
1-1	54	144	143	144	144	253	252	306	0-0
2-0	70	206	201	203	204	314	315	367	1-0
2-1	130	337	335	337	339	450	452	503	2-0
3-0	194	504	527	522	529	647	659	719	0-1
3-1	252	525	540	541	545	652	672	783	3-0
0-2	301	549	560	556	564	698	722	821	1-1
1-2	319	600	641	638	649	723	803	909	2-1
2-2	375	690	791	789	803	792	950	1006	3-1
4-0	380	788	809	810	816	945	965	1064	4-0
4-1	434	816	1017	1014	1032	959	1150	1297	4-1
3-2	480	937	1131	1107	1138	1045	1286	1358	0-2
5-0	627	1030	1138	1133	1149	1152	1323	1451	5-0
4-2	642	1059	1157	1138	1166	1195	1341	1481	1-2
5-1	677	1088	1214	1190	1228	1277	1405	1546	2-2
0-3	809	1136	1315	1296	1335	1284	1495	1606	5-1
1-3	822	1156	1320	1311	1339	1391	1543	1660	3-2
2-3	867	1292	1489	1465	1513	1443	1669	1772	4-2
5-2	866	1345	1524	1523	1541	1524	1687	1838	6-0
6-0	934	1503	1680	1673	1706	1654	1881	1986	6-1
3-3	949	1531	1730	1704	1761	1659	1928	2089	5-2
6-1	980	1571	1910	1839	1926	1685	2108	2243	0-3
4-3	1081	1602	1933	1861	1951	1753	2133	2262	1-3
6-2	1153	1666	1966	1906	1991	1813	2151	2289	7-0
5-3	1270	1709	1979	1961	2002	1877	2167	2342	2-3
7-0	1300	1768	2044	1986	2082	1935	2269	2415	6-2
7-1	1344	1778	2061	2015	2090	2050	2304	2431	3-3
7-2	1503	1939	2105	2094	2140	2105	2324	2435	7-1
6-3	1522	2031	2192	2115	2227	2276	2414	2575	4-3
0-4	1527	2090	2383	2304	2425	2303	2600	2771	5-3
1-4	1538	2190	2428	2394	2476	2339	2623	2779	7-2

Table 1: FEA predictions of resonant frequencies in Hz of a 250×300 mm all-birch 3-ply rectangular plate $3 \cdot 65$ mm thick subject to edge conditions of nominally increasing constraint. SS means simply supported. 50% refers to 'stitched' edge.

A limited comparison can be made between the FEA model and the experimental results shown in Figure 2 above. Table 2 shows fair agreement, where the FEA values are of the SS case of rotation allowed along the line of the respective edge. The two uncertainties are: a) the indefinite values from the experiment and b) the realism of SS to an actual glued edge. Note that the finite element appears to overvalue the low frequency modes and undervalue the highest ones. This could suggest a frequency dependence of the hot melt adhesive, it becoming stiffer at high frequencies – a possible shear thickening behaviour?

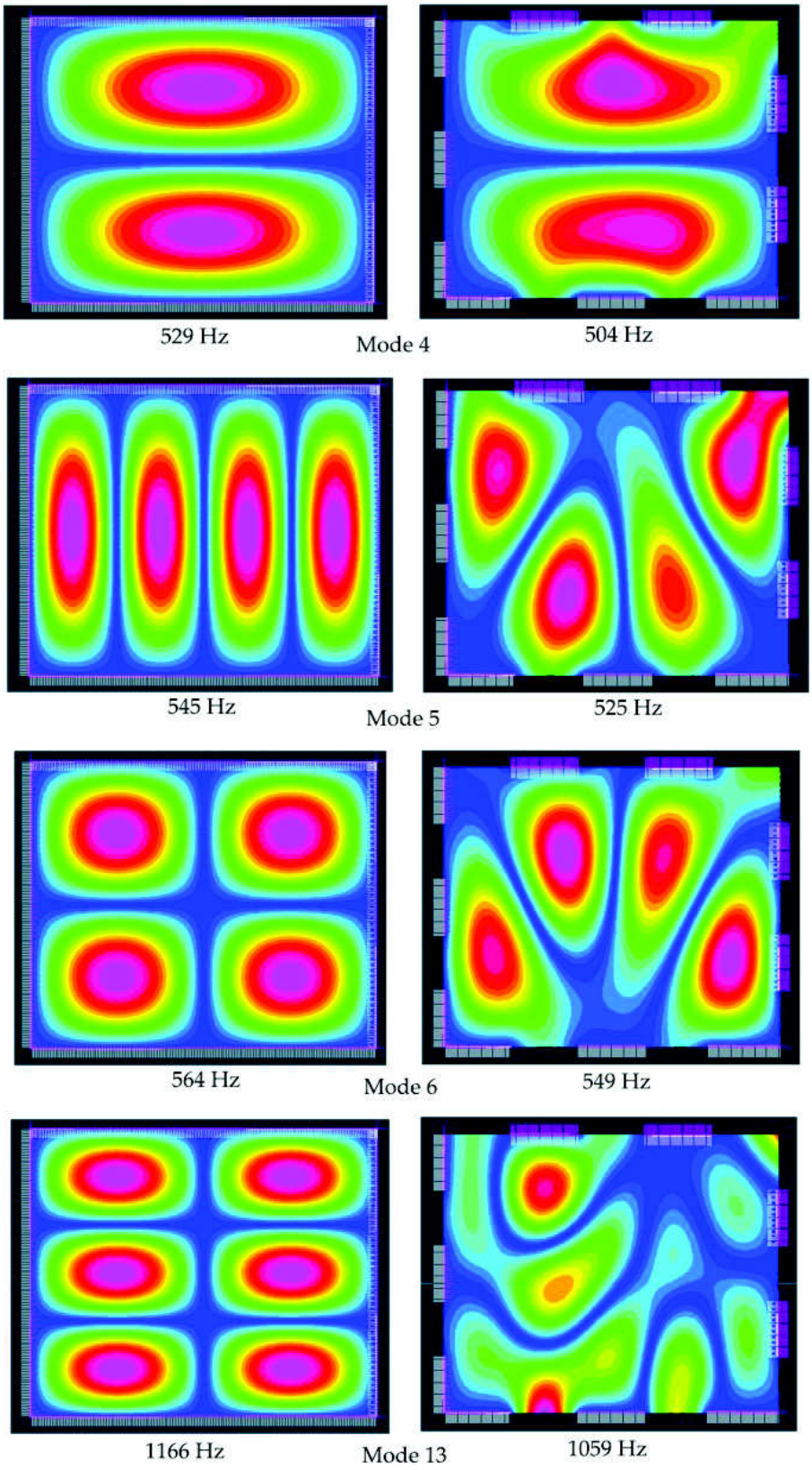

Figure 4: The effect on four normal modes of a rectangular plywood plate of relaxing the edge condition from SS to free along selected lengths of perimeter. Contours of total displacement with blue zero, red maximum.

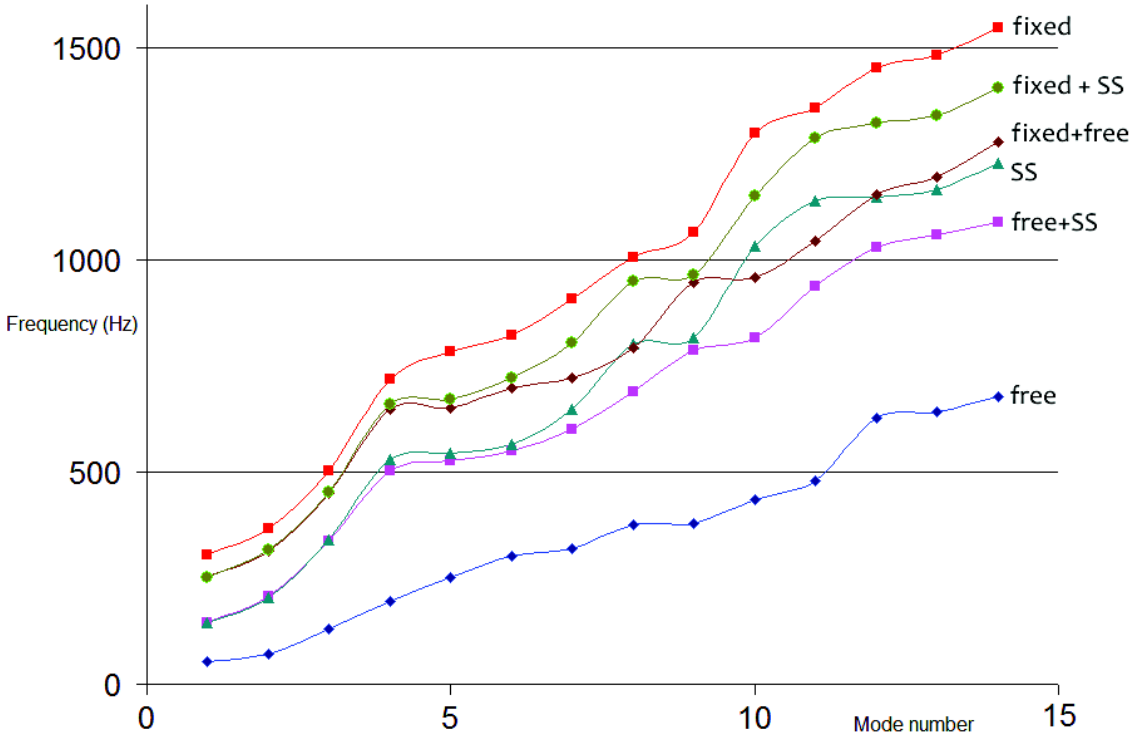

Figure 5: Increase in modal frequency against mode number for various edge constraints.

Mode	Strand7 Hz	Expt Hz
0-0	144	123
1-0	204	212
2-0	339	332 to 385
0-2	529	
3-0	545	
1-1	564	538
2-1	649	643 to 704
3-1	803	
4-0	816	891 to 920

Table 2: Comparison of Strand7 predictions for SS plate compared with experimental measurements on the birch 3-ply plate glued to a frame as shown in Figure 2.

2.3 Constraints within the plate interior

Instead of applying the constraints at the very edges of the rectangular plate, I have examined, by modelling only, the effects of applying them some distance inside the edge. This leaves a ledge of free plate around a constrained interior rectangle. The top left image in Figure 6 shows the modelled 300 by 250 mm rectangle of all-birch 3-ply in blue with the lines of SS constraint as a white rectangle drawn 40mm inside the edge. The other five images are displacement contours for five typical modes. Observe how the constraint separates the plate into two almost independent regions, one inside, one out. The inner rectangle looks like a smaller plate, 220 mm by 170 mm, simply supported around its perimeter. In all modes the nodal lines in the inner rectangle and those over the outer free ledge roughly match up.

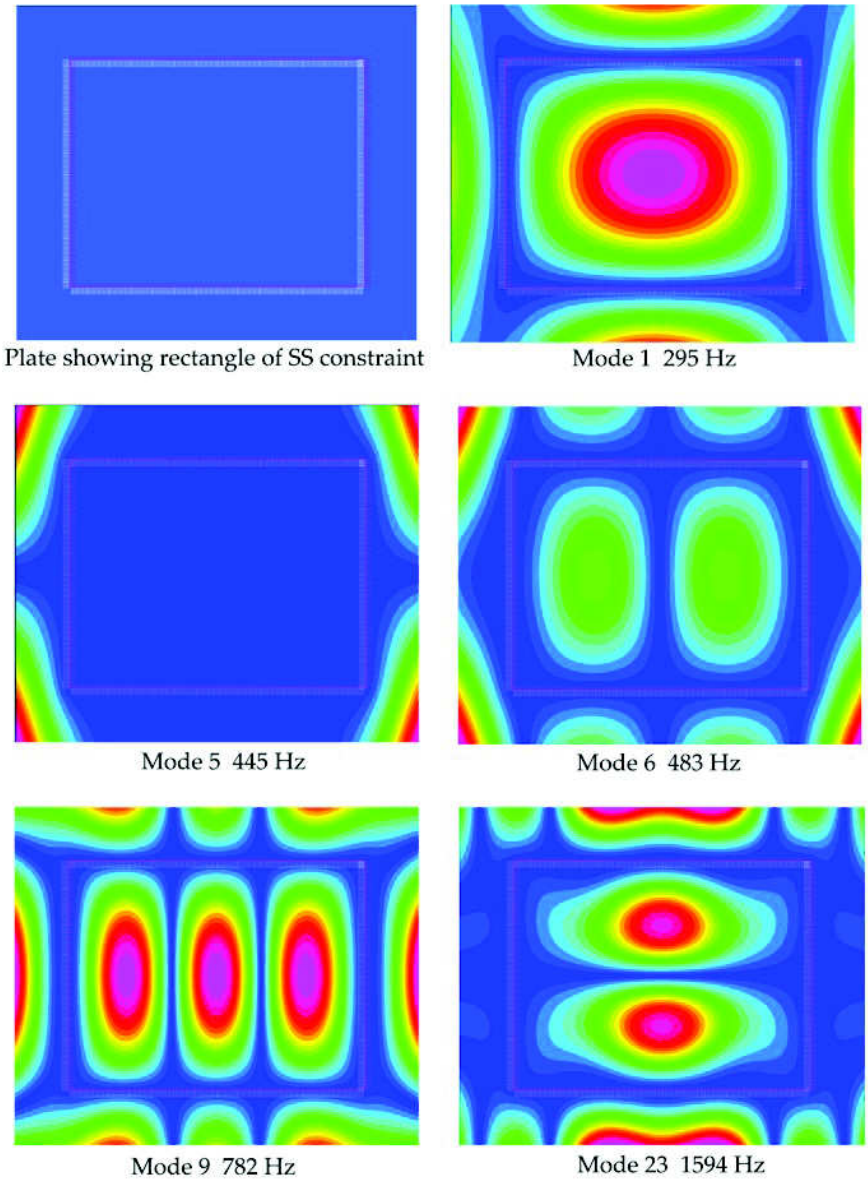

Figure 6: Displacement contours when SS constraint is applied around a rectangle 40 mm interior to the edge of the plate.

Surprisingly, the change in modal frequency as the SS rectangle shrinks towards the centre of the plate is not monotonic. Table 3 gives these frequencies for all distinct modes for distances from the edge of 0 to 80 mm in steps of 10 mm. The left column, 0 mm, is for a SS edge whilst that on the right, 'free', corresponds to the rectangle of constraint having shrunk to a single point.

The values in Table 3 are plotted in Figure 7 to bring out the rich dependence. All modes show an increase in resonant frequency as the constraint is moved a short distance inside the geometric edge. This can be rationalised in terms of the inner rectangle being the only significant vibrating section. As this is smaller is has a high frequency, roughly as $1/(\text{side length})^2$. After about 15 or 20 mm the trend is to falling frequency, as the outer ledge of free plate makes a gradually larger contribution to the overall motion. At 60 mm inside, however, all except the lowest modes show an abrupt increase in frequency. Apart from noting that $62 \cdot 5 = 250/4$, 250 mm being the length of the plate along the grain direction, I have no explanation for this increase.

Mode	0	10	20	30	40	50	60	70	80	free	Mode
0-0	144	172	207	250	295	269	196	148	115	54	1-1
1-0	204	243	293	349	365	270	215	164	131	70	2-0
2-0	339	398	467	513	407	298	357	333	294	130	2-1
0-2	529	622	717	656	445	350	418	375	339	194	3-0
3-0	545	633	730	734	483	464	525	381	354	252	3-1
1-1	564	668	788	759	577	482	527	427	365	301	0-2
2-1	649	770	909	828	615	546	603	484	421	319	1-2
3-1	803	939	1013	885	782	657	719	498	443	375	2-2
4-0	816	949	1099	911	799	747	856	619	549	380	4-0
4-1	1032	1211	1303	1064	900	799	874	629	559	434	4-1
0-2	1138	1313	1329	1079	1034	863	935	802	745	480	3-2
5-0	1149	1326	1505	1212	1081	923	996	807	755	627	5-0
1-2	1166	1363	1530	1272	1112	942	1058	902	874	642	4-2
2-2	1228	1441	1536	1412	1120	950	1125	914	917	677	5-1
5-1	1335	1551	1601	1448	1209	985	1185	1044	964	809	0-3
3-2	1339	1574	1614	1463	1277	1095	1281	1086	1032	822	1-3
4-2	1513	1749	1623	1523	1320	1120	1470	1105	1108	867	2-3
6-0	1541	1778	1696	1655	1444	1130	1495	1186	1301	866	5-2
6-1	1706	1963	1770	1736	1549	1342	1504	1316	1388	934	6-0
5-2	1761	2059	1848	1841	1596	1362	1586	1385	1405	949	3-3
0-3	1926	2225	1912	1871	1650	1418	1622	1472	1437	980	6-1
1-3	1951	2243	1929	1882	1710	1631	1637	1561	1516	1081	4-3
7-0	1991	2258	2074	1913	1716	1638	1773	1586	1568	1153	6-2
2-3	2002	2322	2158	1985	1796	1688	1882	1593	1571	1270	5-3
6-2	2082	2418	2313	2020	1804	1727	1919	1664	1623	1300	7-0

Table 3: Resonant frequencies a 300×250 mm orthotropic plywood plate which is simply supported around a rectangle lying within the various distance (mm) of each plate edge.

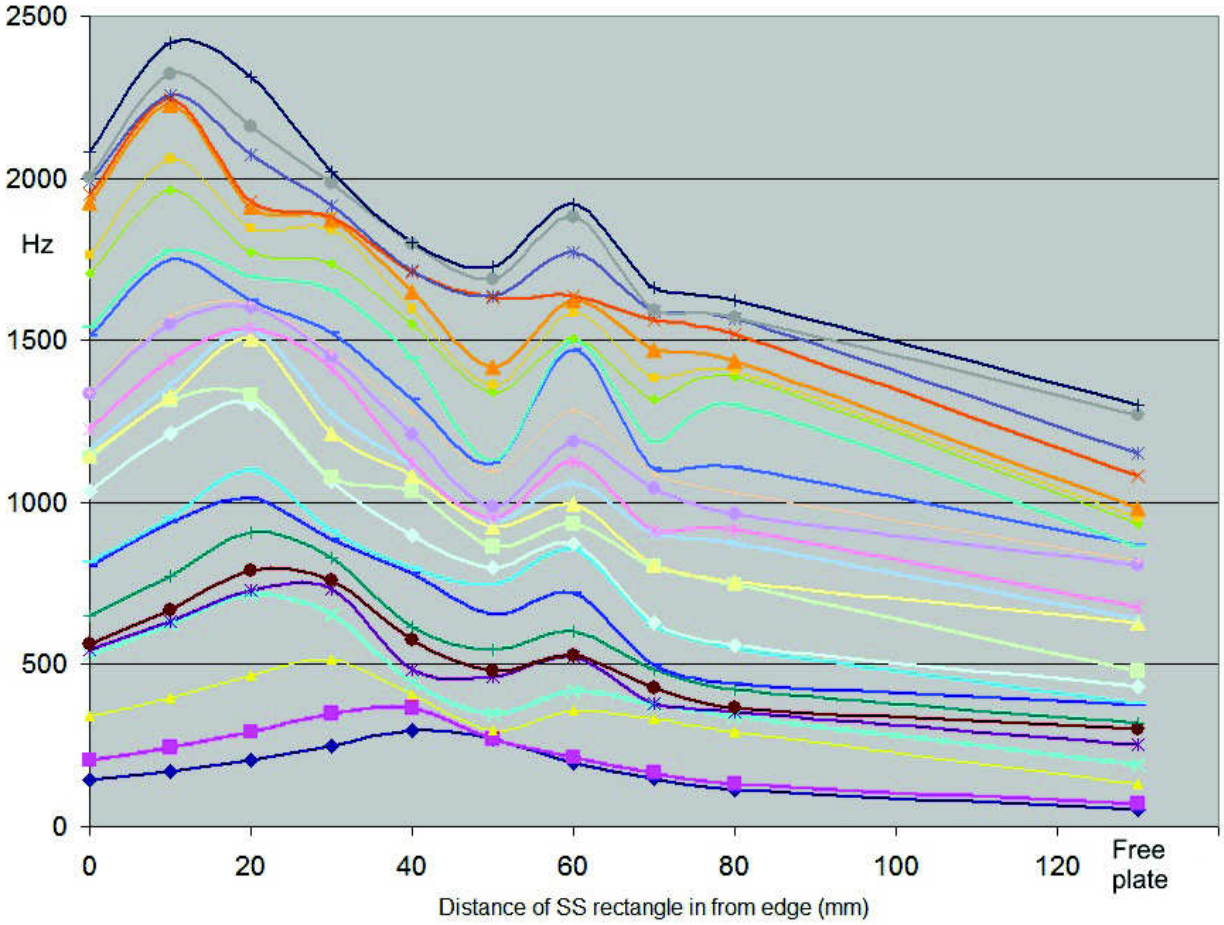

Figure 7: Frequency of normal modes of plate simply supported at various distances from the plate edges. Plot of values in Table 3.

3 Open rectangular box with top plate and ribs only

This project is heading in the direction of understanding the acoustics of the violin and viola through experiment and finite element modelling, so the next stage is to assemble two plates into a box. Many box structures could be modelled through the flexibility of FEA, but I will stick with boxes made from plywood rectangles since these can be most readily fabricated and tested in reality. The first step is to add the side panels (ribs) to the top plate and fasten the free edges of the ribs to a notional fixed, rigid base. Call this structure a lid-only box since it has only the one plate.

In Strand7 I have added ribs to represent 3-ply birch 40 mm deep and $1 \cdot 72$ mm thick ('aeroplane plywood'). These are modelled as 2D shell-plate quad9 elements, each 10 mm square. They share nodes with the top plate along the right-angled edge where they join. This corresponds to a flexible glued joint at which the top and side plates must move together but are otherwise unconstrained. The other edge of each rib (lower in the diagrams) is modelled as simply supported on a fixed, rigid base. Figure 8 shows a close-up of one corner of the box structure. The grain orientation in the ribs is parallel to the short (40 mm) edge. The white square denote the individual elements.

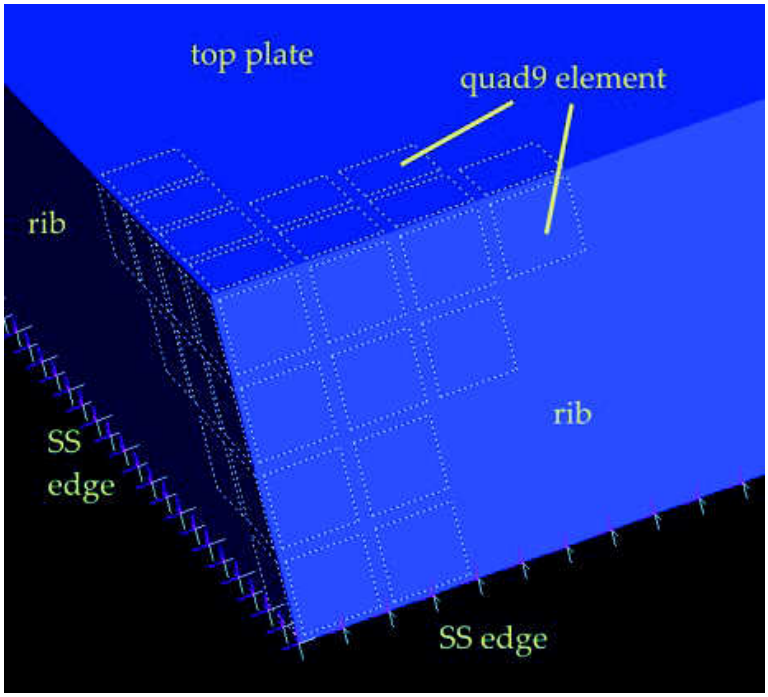

Figure 8: Close-up of one corner of lid-only box made from top plate with four ribs, each rib simply supported at a fixed base.

To see the effects of the ribs it is helpful to compare this lid-only box with the simply supported top plate. With most modes most of the movement is of the top plate; this has displacement contours almost as if it were simply supported except that the frequency has increased. Table 4 compares these frequencies. For completeness the last column lists the equivalent frequencies if the ribs were rigidly fixed to the base. Figure 9 shows two high frequency modes of the box. One can see the simple division of the top plate into equal cells with neighbouring cells vibrating out of phase. There is some modest co-operation of the ribs, with them following the same division into cells as the adjoining top plate.

I also find other types of motion which do not have such similarity to the SS top plate.

1. Figure 10 shows modes 5 and 6 of both the box and the SS plate. The displacement pattern of the box is distorted; it bears a similarity to the images on Figure 5 for the stitched free+SS edge condition, also in modes 5 and 6. I have no ready explanation for this anomaly.

2. Figure 11 shows two modes of a new type in which the ribs participate strongly. Mode 10 is a 'breathing' mode in that the top plate swells up and down like a man's chest. In mode 15 the top plate sways from side to side along the x (cross-grain) axis as the ribs hinge about the y (shorter) sides.

3. In mode 27 at 2056 Hz the top plate rotates about the thickness axis as the ribs twist.

From the point of view of the violin, modes involving mainly in-plane motion of the plates cannot contribute to sound radiation, but they may be important by wastefully taking energy from the radiative modes – those with significant transverse velocity.

Mode	SS plate	SS ribs	fixed ribs
0-0	144	186	193
1-0	204	257	263
2-0	339	400	407
0-2	529	568	575
3-0	545	611	619
1-1	564	610	619
2-1	649	704	713
3-1	803	865	875
4-0	816	885	896
breathe		1040	1077
4-1	1032	1098	1112
0-2	1138	1170	1180
5-0	1149	1216	1221
1-2	1166	1201	1212
sway in x		1245	1281
2-2	1228	1267	1279
5-1	1335	1399	1416
3-2	1339	1383	1397
4-2	1513	1561	1579
6-0	1541	1602	1624

Table 4: Modal frequencies in Hz of the lid-only box with SS ribs compared to the SS plate.

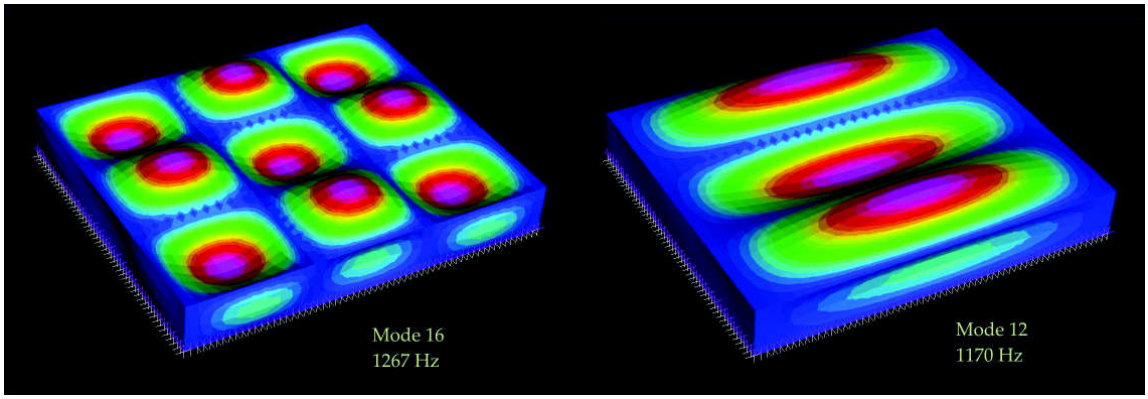

Figure 9: Two higher modes of the lid-only box showing participation of the ribs in the plate mode.

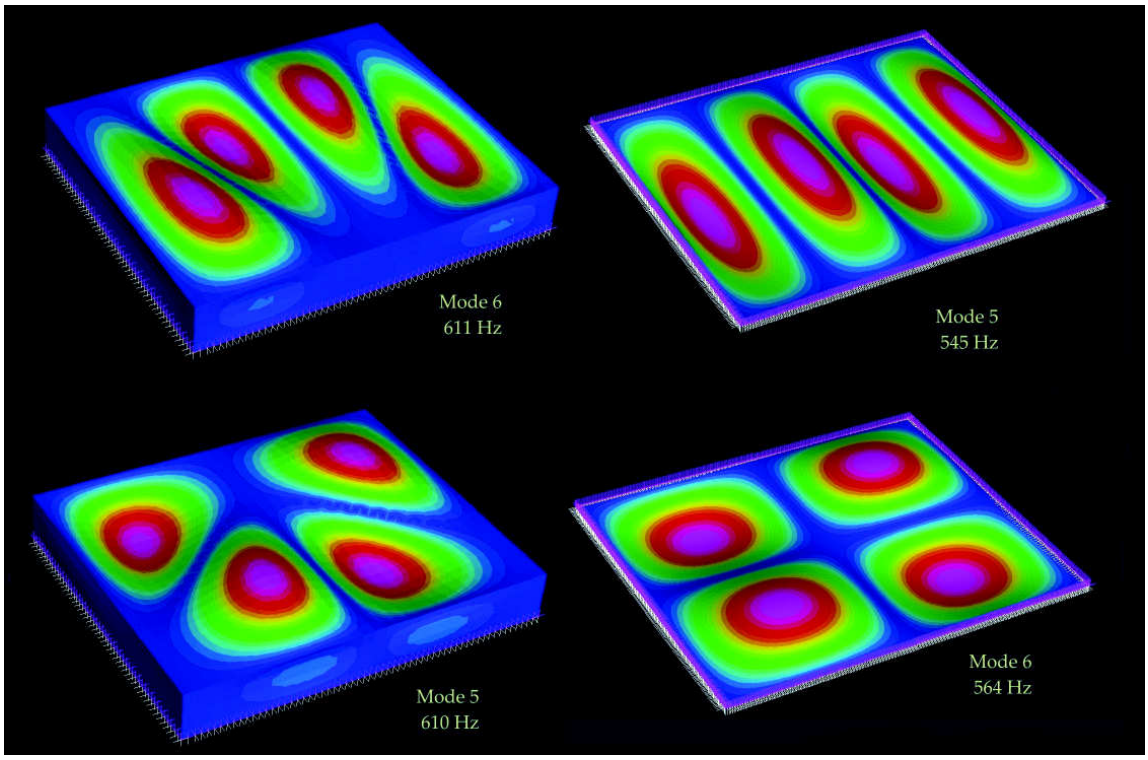

Figure 10: Two modes of the lid-only box compared with the corresponding modes in a SS plate.

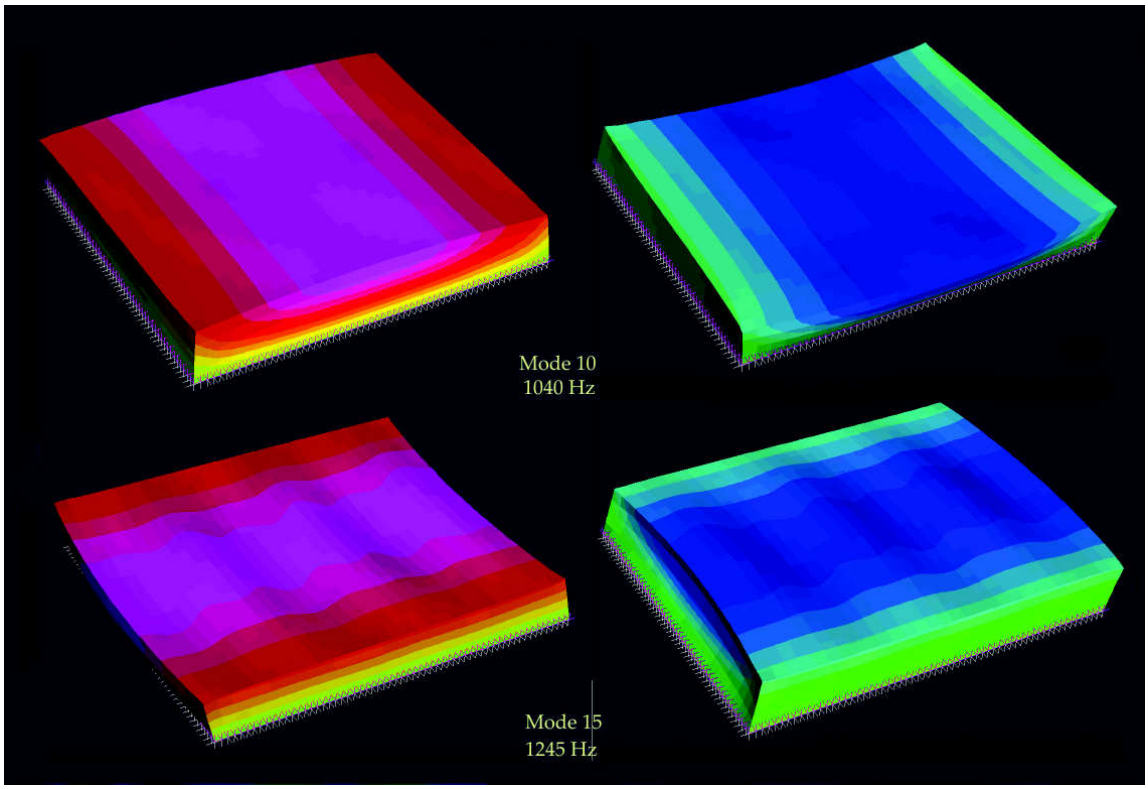

Figure 11: Two modes of the lid-only box having no counterpart with a single plate. Mode 10, a breathing mode, Mode 15 a swaying mode. The two extremes of motion are shown in each case.

4 Closed rectangular box

4.1 Coupling of two vibrating plates

Before we enter into the nitty-gritty of the vibrations of a closed wooden box, it is helpful to bear in mind that we are taking two plates, each with its own vibrational modes, and coupling them together via the box sides. Though this is a complicated case of coupled oscillating systems, we can gain insight from the simplest model of two coupled harmonic oscillators.

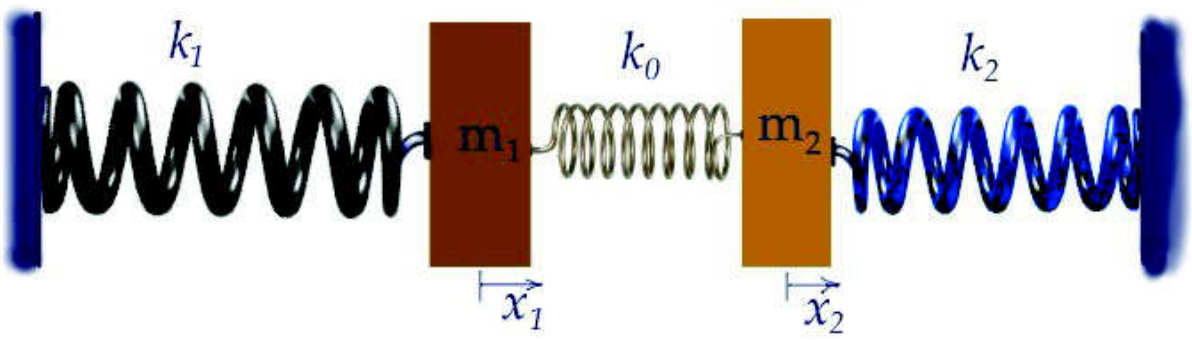

Figure 12: Two mass-and-spring oscillators coupled by a central spring, stiffness k_0.

Consider the arrangement in Figure 12 of two simple mass-and-spring oscillators, m_1, k_1 and m_2, k_2, coupled by a spring with stiffness constant k_0. The system has two degrees of freedom, being the displacements x_1 and x_2 from equilibrium. If we take the left hand oscillator in isolation, a displacement x_1 produces a force $-k_1x_1$ and this equals $m_1\ddot{x}_1$ by Newton's second law. We look for harmonic solutions of the form $x_1 = A_1\cos(\omega t)$ and so arrive at the quadratic relation for natural frequency

$$\omega_1^2 \;=\; \frac{k_1}{m_1}, \tag{1}$$

and similarly for the right hand oscillator in isolation. We can take $\omega_1 \le \omega_2$. The central spring couples these equations of motion:

$$\begin{aligned} m_1\ddot{x}_1 &= -k_1x_1 + k_0(x_2 - x_1) \\ m_2\ddot{x}_2 &= -k_2x_2 - k_0(x_2 - x_1) \end{aligned} \tag{2}$$

Again look for harmonic solutions and recast the above simultaneous differential equations as linear equations in matrix form:

$$\begin{pmatrix} k_1 + k_0 - m_1\omega^2 & -k_0 \\ -k_0 & k_2 + k_0 - m_2\omega^2 \end{pmatrix}\begin{pmatrix} A_1 \\ A_2 \end{pmatrix} \;=\; \begin{pmatrix} 0 \\ 0 \end{pmatrix} \tag{3}$$

The condition for a non-trivial solution is that the determinant of the coefficient matrix be zero:

$$(\omega^2)^2 m_1m_2 \;-\; \omega^2[k_0(m_1 + m_2) + k_1m_2 + k_2m_1] \;+\; [k_0(k_1 + k_2) + k_1k_2] \;=\; 0, \tag{4}$$

which is a quadratic in ω^2. This can be simplified a little by dividing by m_1m_2 and writing in terms of the natural frequencies of the uncoupled oscillators:

$$\omega^4 \;-\; \omega^2\left[k_0\left(\frac{1}{m_1} + \frac{1}{m_2}\right) + \omega_1^2 + \omega_2^2\right] \;+\; \left[\frac{k_0}{m_2}\omega_1^2 + \frac{k_0}{m_1}\omega_2^2 + \omega_1^2\omega_1^2\right] \;=\; 0. \tag{5}$$

The exact solution is straightforwards but messy and quite opaque. Two limiting cases are more enlightening. First, if the coupling is weak, the two solutions can be expanded as power series in k_0 as follows:

$$\omega_-^2 \approx \omega_1^2 + \frac{k_0}{m_1} - \frac{k_0^2}{m_1 m_2}\left(\frac{1}{\omega_2^2 - \omega_1^2}\right), \qquad \omega_+^2 \approx \omega_2^2 + \frac{k_0}{m_2} + \frac{k_0^2}{m_1 m_2}\left(\frac{1}{\omega_2^2 - \omega_1^2}\right). \tag{5},$$

where the + and −1 subscripts denote the sign of the square root. These are valid provided $\omega_1 \not\approx \omega_2$. They show that for $\omega_2 > \omega_1$ the higher frequency increases, while the lower one either increases or decreases according to whether

$$\frac{k_0}{m_2}\left(\frac{1}{\omega_2^2 - \omega_1^2}\right) < 1 \quad \text{or} \quad > 1.$$

So very weak coupling causes a slight increase is both natural frequencies. If $k_0 = m_2(\omega_2^2 - \omega_1^2)$, then $\omega_- = \omega_1$. If $\omega_2 \to \omega_1$, ω_+ will decrease, meaning that two natural frequencies that are close to each other will be pushed apart by the coupling.

The second special case is when $\omega_2 \approx \omega_1$ and the coupling is not weak, as is the case with a violin. If the frequencies are actually equal – for instance, if the two wooden plates of a box have been tuned to each other – then the solutions direct from Eq 3 are

$$\omega_-^2 = \omega_1^2, \qquad \omega_+^2 = \omega_1^2 + k_0\left(\frac{1}{m_1} + \frac{1}{m_2}\right). \tag{6}$$

More generally, if $\omega_2^2 - \omega_1^2 = \epsilon$, the Taylor expansion in ϵ begins

$$\omega_-^2 = \omega_1^2 + \epsilon\left(\frac{m_2}{m_1 + m_2}\right) - \ldots, \qquad \omega_+^2 = \omega_1^2 + k_0\left(\frac{1}{m_1} + \frac{1}{m_2}\right) + \epsilon\left(\frac{m_1}{m_1 + m_2}\right) + \ldots. \tag{7}$$

In fact the first of these can be written

$$\omega_-^2 = \frac{k_1 + k_2}{m_1 + m_2} - \ldots > \omega_1^2 \text{ if } \epsilon > 0.$$

The amplitudes, or rather the amplitude ratio A_1/A_2, can be found by substituting the frequencies into Eq 3. However, note that when this determinant is zero, the two rows are merely multiples of one another. Therefore at either frequency

$$\frac{A_1}{A_2} = \frac{k_0}{k_1 + k_0 - m_1\omega_\pm^2} = \frac{k_2 + k_0 - m_2\omega_\pm^2}{k_0}. \tag{8}$$

In the case where the two oscillators have the same frequency (Eq 6), this ratio readily simplifies to 1 at the lower frequency and to $-m_2/m_1$ at the upper, whatever the strength of coupling. The signs + and − here are important; they mean that the two masses move in the same direction at the lower frequency and in opposite directions at the higher. Applying this to the wooden plates of a box, 'same direction' must be interpreted as both moving away from the ribs, while 'opposite direction' means that one plate moves towards the ribs while the other is moving away. These, therefore, are the well recognised symmetric (lower frequency) and antisymmetric (higher) modes. In the symmetric mode the two plates move much as they would do if not coupled.

4.2 Comparison between experiment and LISA 8 FE model

In 2013 I was privileged to have a pre-release copy of the Canadian finite element program LISA 8, which has the capability to model orthotropic materials, not shared with LISA 7. I therefore constructed a box of the pink-red hardwood 3-ply, $2 \cdot 91$ mm thick, to make a comparison between measured resonant frequencies and those predicted by LISA 8. This material has been described and characterised in a companion article 'The orthotropic elastic constants and vibrational modes of plywood plates by experiment and finite element analysis', also published on the mathstudio.co.uk web site. The box, a simple cuboid, was made with dimensions similar to those of a violin – length 34 cm, width 16 cm, depth $4 \cdot 5$ cm. The grain was parallel to the long side on each of the six faces. To support the sides onto the base during construction, I glued a triangular prism of wood, side about 1 cm, into each short corner. Other than that, all joints were simple glued butt joints between the plywood edges.

The usual procedure was followed to determine the normal modes, namely spectrum analysis of about eight recorded tap sounds followed by Chladni figures at the spectral peak frequencies. The electro-magnetic acoustic vibrator was used to excite the Chladni figures, sometimes by placing the box on the upturned vibrator, sometimes placing the vibrator downwards on top of the box. I found that the most readily generated modes were some amongst the high frequency ones. At some peak spectral frequencies no single, distinct pattern, stable again small positional changes of the vibrator, could be found. Moreover, at low frequencies where there are few node lines, a convincing Chladni figure could not be found. Instead, I found that the box acted as an effective acoustic amplifier. For instance, the tap tone spectra consistently showed a strong peak at about 318 Hz. When the vibrator, placed by itself on the table, was driven at this frequency, its fairly quiet note could be heard, but as soon as the box was rested upon it, the sound became suddenly very loud. However, no convincing Chladni figure appeared.

Figures 13 and 14 show photographs of the Chladni figures up to 1222 Hz. Each frequency is at or close to a peak in the tap sound spectra, though I cannot guarantee that each is a single, distinct mode of vibration. Where more than one figure could be found at a given frequency, both are presented.

LISA 8 was first compared with Strand7 in modelling the normal modes of a plate of this pink-red 3-ply. They agree within 1 or 2 Hz at all frequencies except the lowest, for which Strand7 predicted 55 Hz and LISA 66 Hz. I cannot explain this discrepancy, but otherwise the agreement was very good, enough to give confidence in using LISA 8. The LISA mesh was created with hex8 shell elements, 36 by 16 by 4 in number. The corner stiffeners were modelled by similar hex8 elements diagonally across the short corners. The elastic constants were those determined in a previous article: $E_1 = 9 \cdot 44$, $E_2 = 4 \cdot 06$, $G_{12} = 1 \cdot 04$, $G_{23} = 0 \cdot 51$, $G_{31} = 0 \cdot 25$ GPa, $\nu_{12} = 0$. A similar mesh was made without the corner stiffeners to gauge their effect; the lower frequencies differed by 1 to 3 Hz, and the higher frequency ones between 1 and 10 Hz – not really significant.

The displacement contours of the top plate are shown in Figures 15 and 16 for the box with stiffened corners. These contours are on a temperature scale in which the dark red is zero, so these red lines should correspond with the experimental Chladni figures. There is a broad similarity between the predictions of the finite element model and the experiment, though not the striking agreement seen with some single flat plates. There certainly are pairs of modes which give a similar pattern of node lines on the box top, such as at 291 and 377 Hz, and 525 and 609 Hz. These must be the symmetric and antisymmetric pair, but it is not possible using only Chladni figures to tell them

apart. Based on the order of the modes and similarity of frequency, my judgement of the match between model and experiment is that in Table 5. Overall I find the results satisfactory.

Expt Hz	LISA 8 Hz	Expt Hz	LISA 8 Hz
	235	807	836
300	334	906	880
325	339	870	918
393	418	945	951
525	536	1041	1071
609	605		1080
645	645	1157	1143
	667		1161
750	719	1222	1224
750	720		1274

Table 5: An attempt to match the resonant frequencies of the plywood box, as measured and computed.

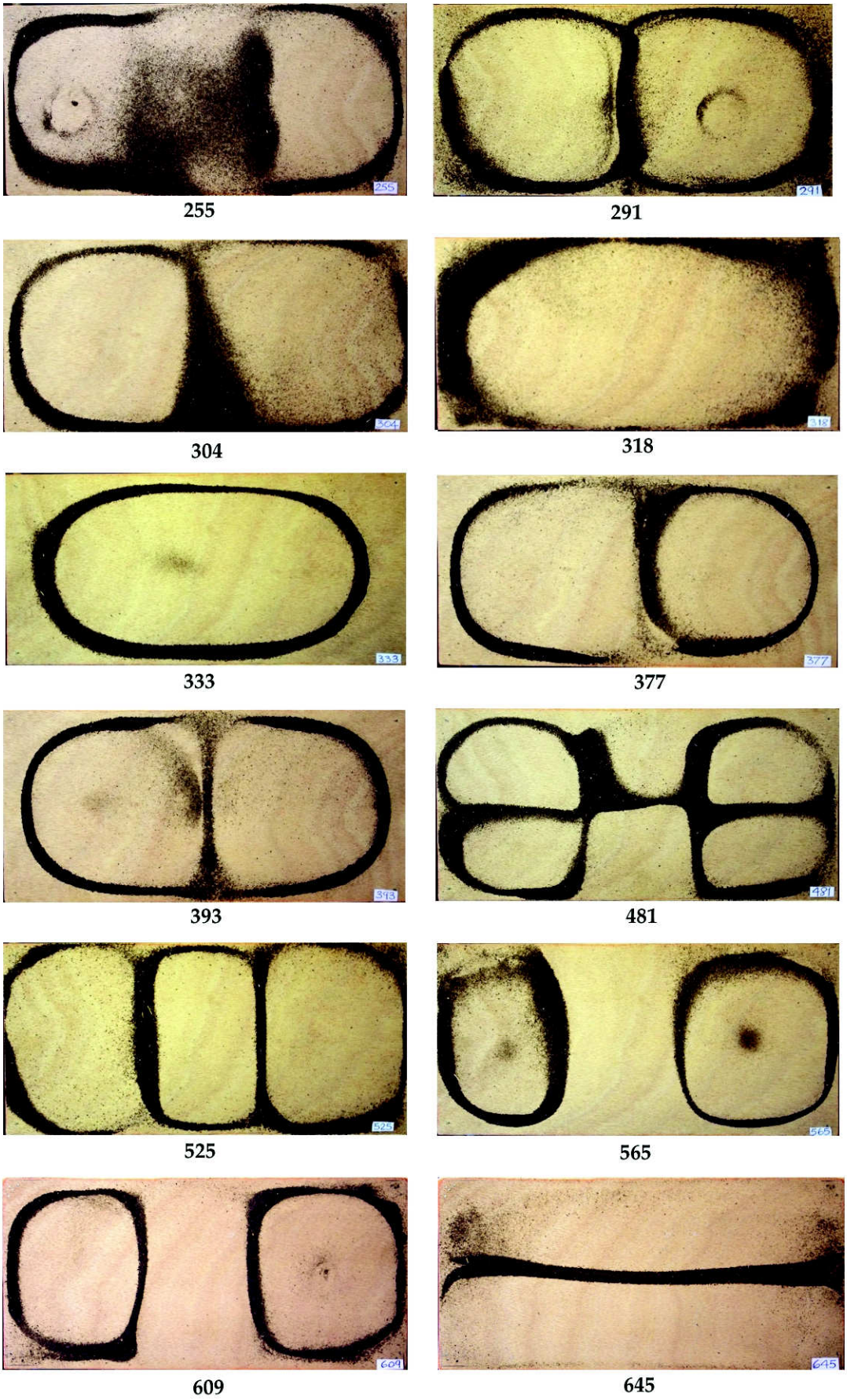

Figure 13: Chladni figures on the top plate of a rectangular box; lower frequencies.

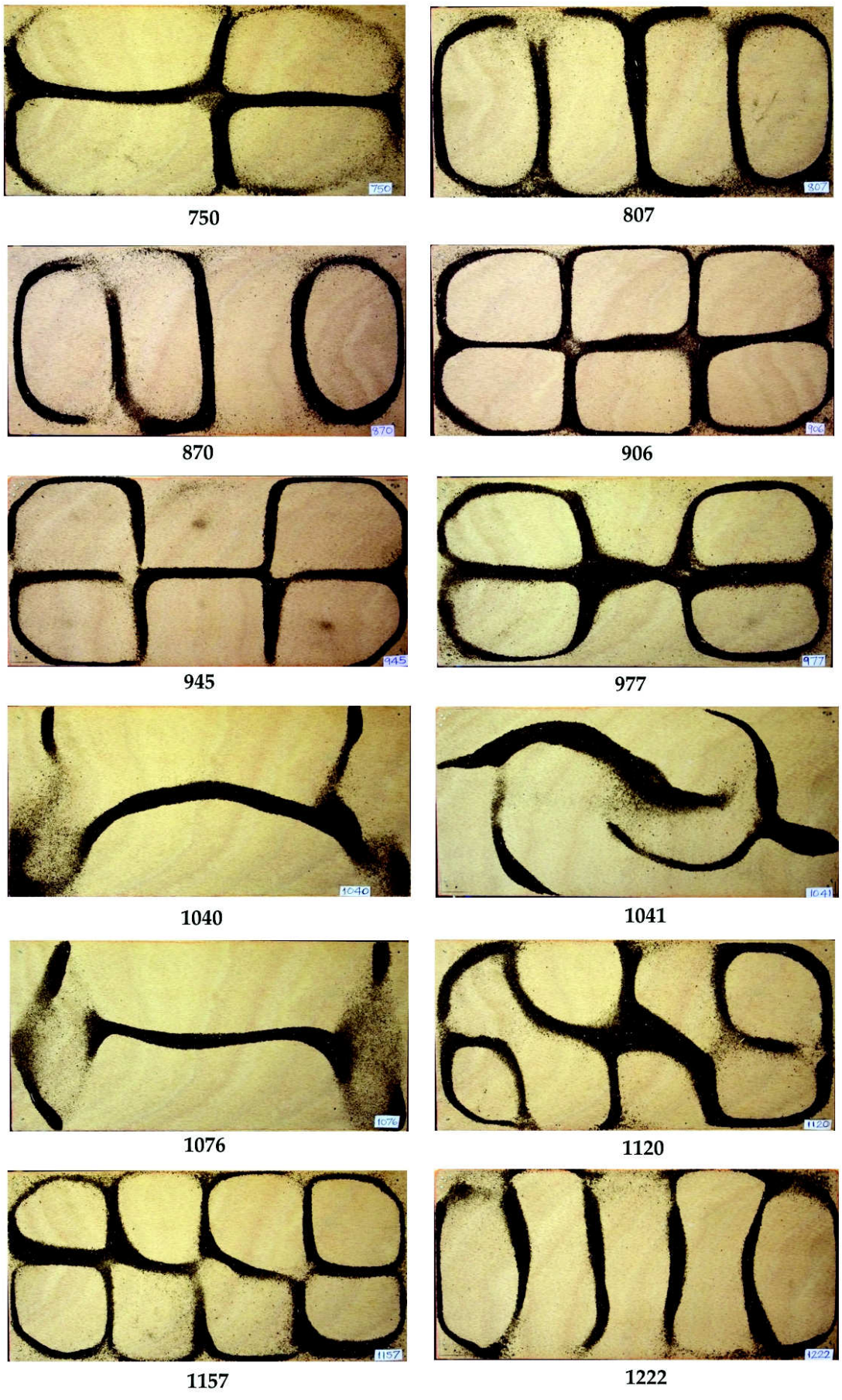

Figure 14: Chladni figures on the top plate of a rectangular box; higher frequencies.

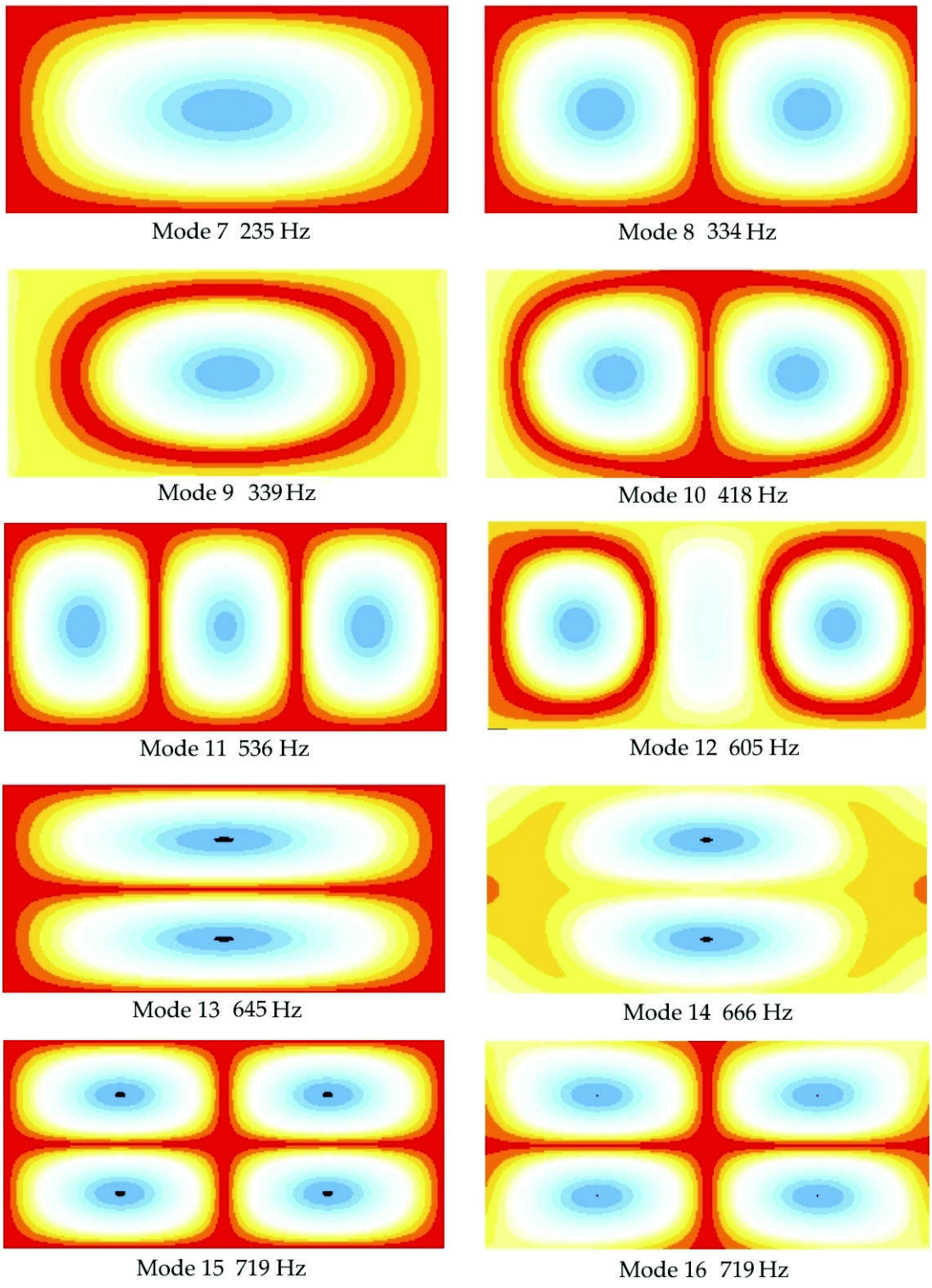

Figure 15: Contours of displacement in the top plate of the cuboidal box. Lower frequency modes as predicted by LISA 8. Red is zero displacement, blue maximum. (The first 4 modes are deformation-free translations and rotations, and so are not shown.)

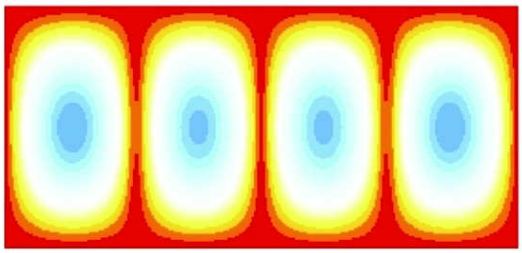

Mode 17 836 Hz

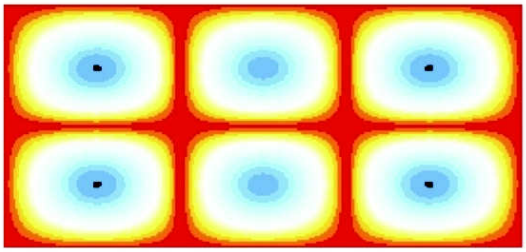

Mode 18 880 Hz

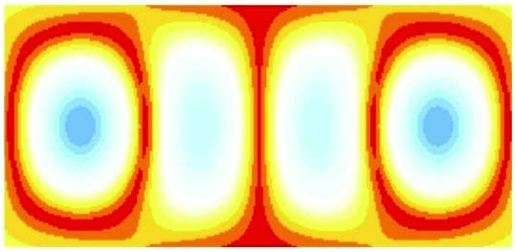

Mode 19 918 Hz

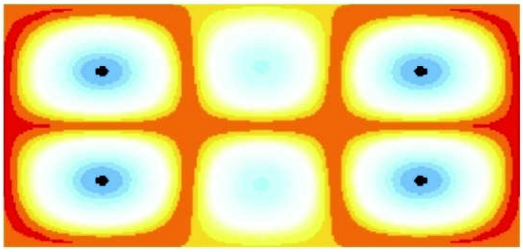

Mode 20 951 Hz

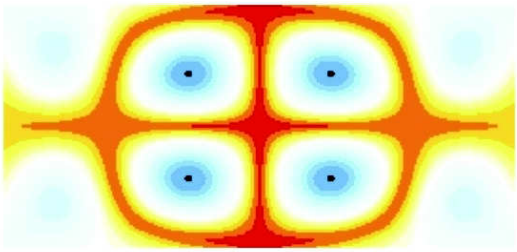

Mode 21 1071 Hz

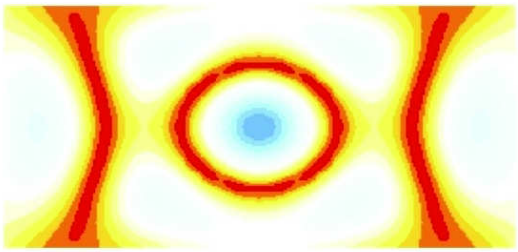

Mode 22 1080 Hz

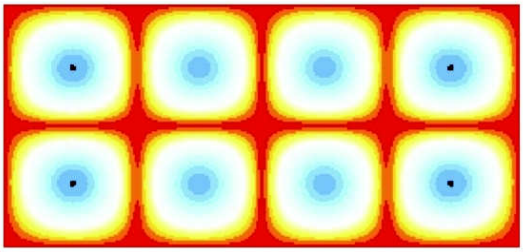

Mode 23 1143 Hz

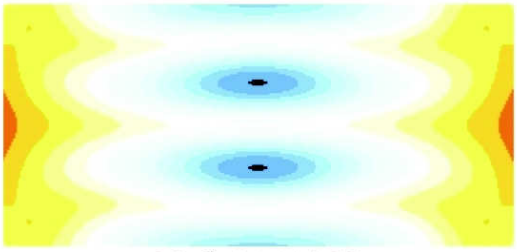

Mode 24 1161 Hz

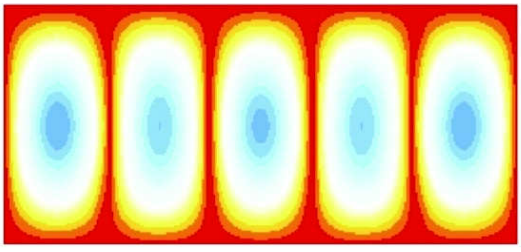

Mode 25 1224 Hz

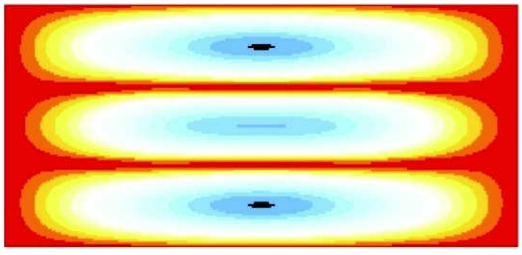

Mode 26 1274 Hz

Figure 16: As Figure 28, except higher frequency modes as predicted by LISA 8.

4.3 Finite element model of box in Strand7

The remainder of this article deals with Strand7 models of a box based on the 300 by 250 mm birch 3-ply plates already discussed at length in §2 and 3. There is no further comparison with experiment.

In the finite element model the back plate is fitted to the ribs by copying the top plate to the position of the back, then fusing the mesh nodes around its perimeter to the nodes on the ribs. A thickness is assigned to these 2D shell-plate finite elements, which determines their masses. We can therefore model the effect of having the top and back plates with different thicknesses and hence resonant frequencies. There is much written, and even more anecdotal discussion, about the tuning of violin plates by wood removal before they are assembled into the violin belly. One web site (www.kreitpatrick.com) typically states

> When the top and back plates have the same coupling frequency, the bow cannot cope with the dynamics and power of the instrument: the strings saturate. This explains why Stradivarius and Guarneri tuned the coupling frequency of the back plate one half-tone to one tone above that of the top plate. On the finest Italian violins, the delta between these two frequencies averages 25 Hz.

I interpret this as follows: if the two plates have the same normal frequencies, the violin as a whole will resonant strongly at certain frequencies but be quite unresponsive in between resonances. In playing a musical scale it would be almost impossible to maintain an even loudness and tone with the bow. By making the top and back plates about one or two semitone tones apart, some 6% to 12% difference in frequency, the energy uptake from the bow can be distributed more evenly across the instrument's compass. This of course assumes that the various constraints in the completed instrument do not impose their own changes on resonance.

There are many ways in which the top and back plates of a violin family instrument could be given different resonant frequencies:

- changing the plate thickness, either uniformly or by tapering,
- changing the elastic constants by changing wood grain orientation,
- changing elastic constants by changing material, *e.g.* a different species of wood or plywood,
- adding a stiffening bar such as the bass bar fitted to the underside of a violin top plate,
- making the plates of unequal size, though this would mean that the ribs were no longer at right angles to the two plates,
- making the plates different shapes, again with changes to the ribs to accommodate this.

In addition, the resonances of the whole box can be changed by

- changing the depth, thickness and/or grain orientation of the ribs,
- wedging a sound post between the plates at one of many possible positions,
- changing the glued seams between plate and ribs, for instance to an alternating 'stitched' scheme,
- gluing stiff blocks of wood between the plates at a few places round the perimeter, as happens in actual violins.

In principle the normal modes under all of these changes could be studied by FEA and experimentally and in the next section, §5, I examine five types of variation. We have to bear in mind, however, that determining the normal modes is only one step towards studying the sound quality of a musical instrument; in addition one needs the dynamic response to forced vibration of the bridge, and the radiation of sound to the listener from the vibrating box and internal air cavity via the f-holes. Moreover, the requirements for stability under the static load of the strings, plus the ergonomics of playing and the practicalities of manufacture may rule out some of the above options. Nevertheless, it is probably worth examining the extent to which the various resonances of the box can be controlled and adjusted to fall at roughly equal pitch increments, as this seems to be what violin makers attempt to do. We might expect that n different changes would need to be made to adjust n resonant frequencies to particular values.

The case in which both plates are identical is the reference case for all such variations to box structure, so let us deal with that now. The plate thicknesses have both been set to $3 \cdot 65$ mm, the ribs' to $1 \cdot 72$ mm, and the elastic constants are for the all-birch 3-ply with surface grain in the y direction, parallel to the shorter side. Because the two plates are identical, they will have the same resonances and the displacements will either in the same or the opposite sense. The position is similar to Lamb waves in a plate, where symmetric and antisymmetric modes are distinguished. In the symmetric the displacements of each plate at corresponding points are either both towards or both away from the central plane midway between the plates. This causes the box locally to shrink or expand in the thickness dimension. In the antisymmetric cases the two plates move pointwise in the same direction, causing the box to flex and ripple.

There is some scope in modelling with Strand7 to apply constraints to eliminate modes which cause only body translation or rotation without distortion. There are six of these altogether. For single plates I have found that constraining one central point in x and y eliminates translations in the x and y directions without distorting the displacement contours in the z direction. This would leave four modes without distortion, and hence of no interest. In the case of a box I find consistency of modal frequencies in two cases:

1. the box free of all constraints,
2. the box supported at the four corners of the bottom plate on highly compliant spring-like beam elements, the other ends of which are fixed in position by free to rotate.

The displacement contours agree in both cases for all symmetric modes. For antisymmetric ones the free box (1) does not show quite the same displacements in the two plates, but the spring-supported case (2) does. I have therefore taken this as definitive.

Table 6 lists the normal modes of the box, identifying them as either symmetric (S) or antisymmetric (A). Most can be recognised as an $(m - n)$ type, very similar to a simply supported plate, though some such as XX at 999 Hz are new (Figure 18). Some of the high frequency A modes have the form of small scale structure superimposed on large scale bending or twisting of the box. 'Egg box' in the comments column indicates that the short scale displacement dimples the plate into alternate hill and hollows like the familiar cardboard egg box. The nature of these modes is best seen in an animation, but some impression may be gained from the images in Figures 17 to 20. In Table 7 some modes have been sorted into type, S or A. The second column gives the counterpart in a single SS plate, from Table 1. In all cases the box S modes have a higher frequency than their single plate SS counterpart, indicating greater constraint, but the A modes are sometimes higher, sometimes lower. The simple harmonic oscillator theory of §3.1, which predicts that S will have a lower frequency than A, seems to apply only at low frequencies.

box				single
				SS plate
Hz	symmetry	mode	comment	Hz
177	S	0-0	breathe	144
247	S	1-0		204
263	A	0-0	dish	
320	A	1-0		
388	S	2-0		339
461	A	2-0		
498	A	1-1	twist	
518	A	2-1		
558	S	0-1		529
598	S	3-0		545
599	S	1-1		564
662	A	3-0		
675	A		bend & dish	
691	S	2-1		649
754	A	2-1		
775	A	3-1 mod		
850	S	3-1		803
870	S	4-0		816
968	A	0-3		
999	A	XX	double X	
1011	A	3-1	twist & egg box	
1022	A	4-0		
1081	S	4-1		1032
1126	A	4-1		

Table 6: Reference case of a rectangular box with both plates $3 \cdot 65$ mm thick. Box compared with the modes of a simply supported single plate. S, A denote symmetric and antisymmetric mode type. $m-n$ mod indicates a form similar to $(m-n)$ but with superimposed displacements.

mode	single SS plate	box S	box A
0-0	144	177	263
1-0	204	247	320
2-0	339	388	461
3-0	545	598	662
4-0	816	870	1022
1-1	564	599	498
2-1	649	691	518
3-1	803	850	775
4-1	1032	1081	1126

Table 7: Frequency values (Hz) of Table 5 sorted by $(m-n)$ mode type.

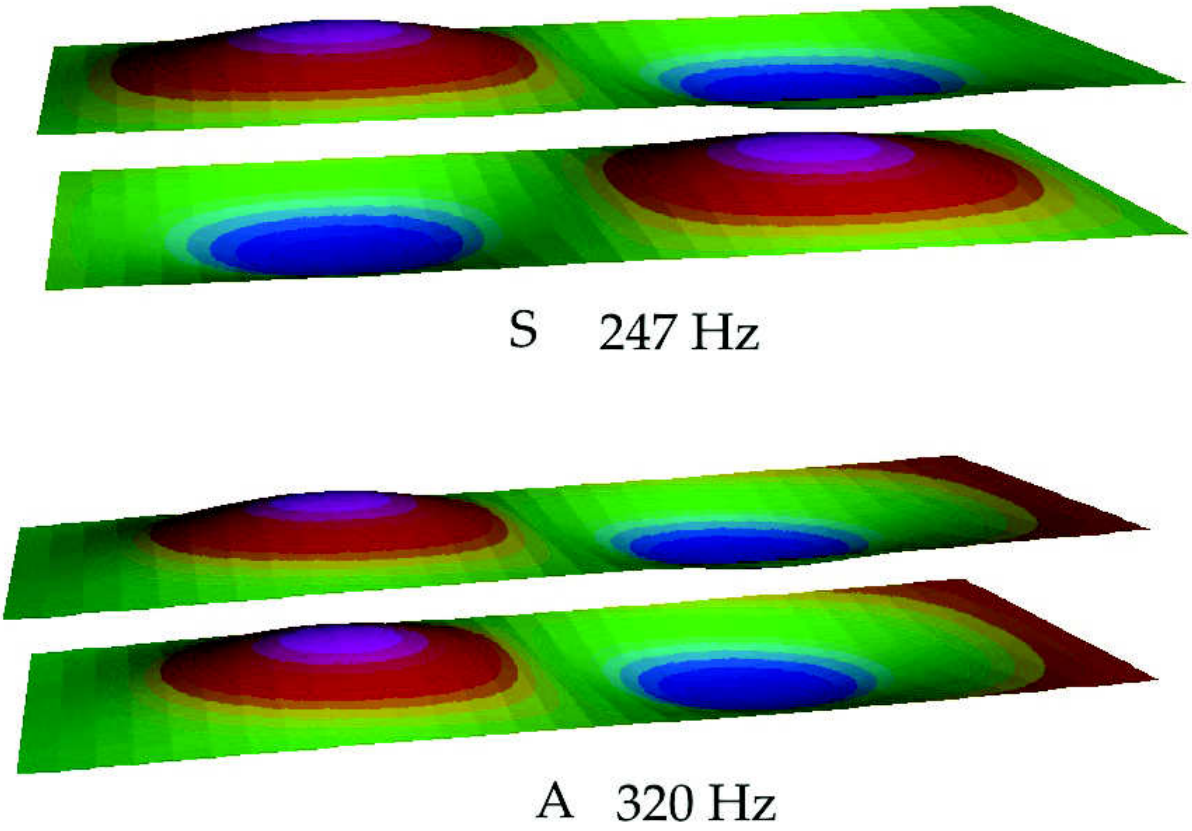

Figure 17: Contours of z displacement for the symmetric and antisymmetric two (0-1) modes. The ribs are present but invisible. Red = max. up, blue = max. down

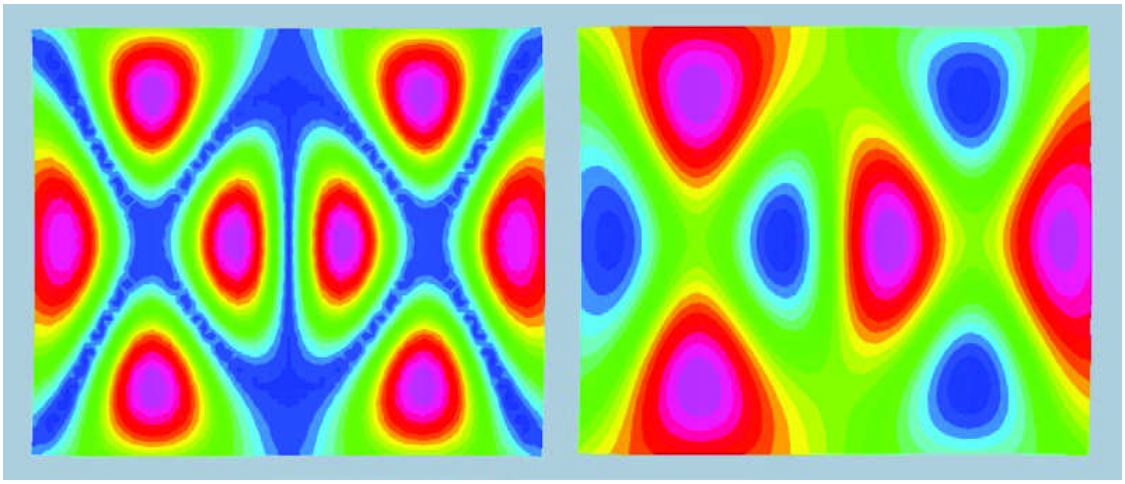

Figure 18: The antisymmetric XX mode at 999 Hz. Left image shows contours of total displacement with blue = 0, red = maximum. Right panel shows only the z displacement with red = max. up, blue = max. down. The wood grain is vertical in the images, and both plates have the same displacements.

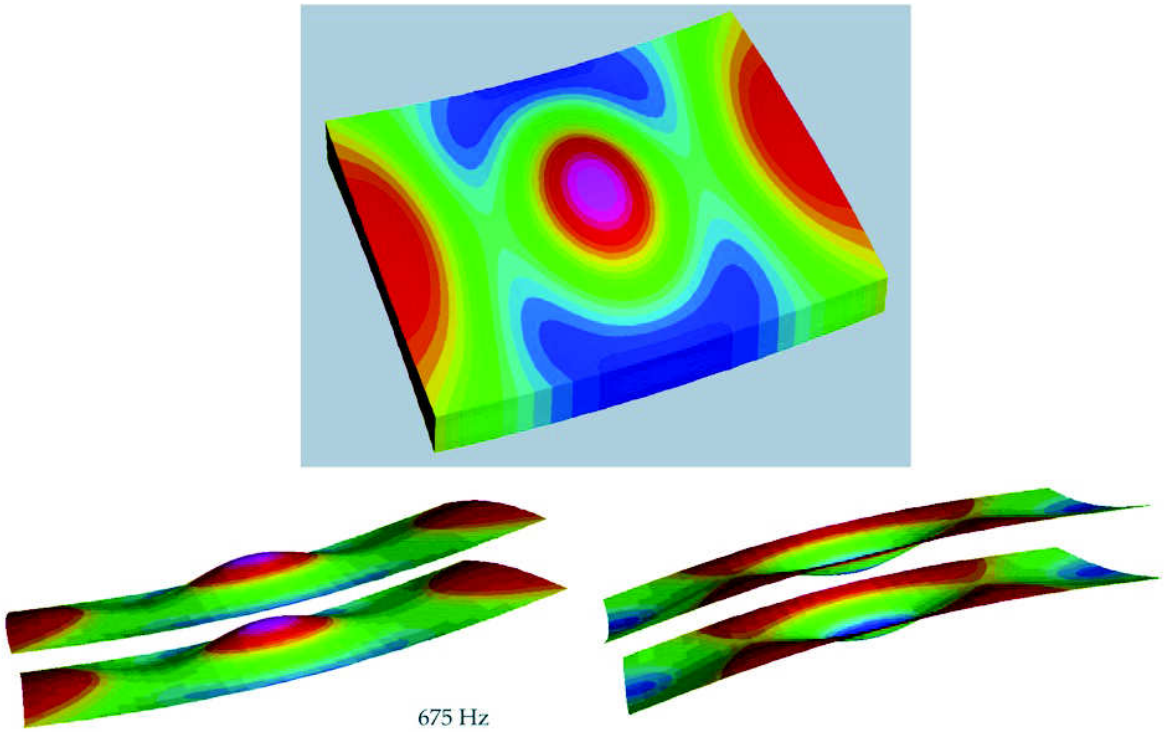

Figure 19: Contours of z displacement from two views onto the antisymmetric box mode at 675 Hz. The lower panel shows the extremes of motion and the bend. Red = max. up, blue = max. down.

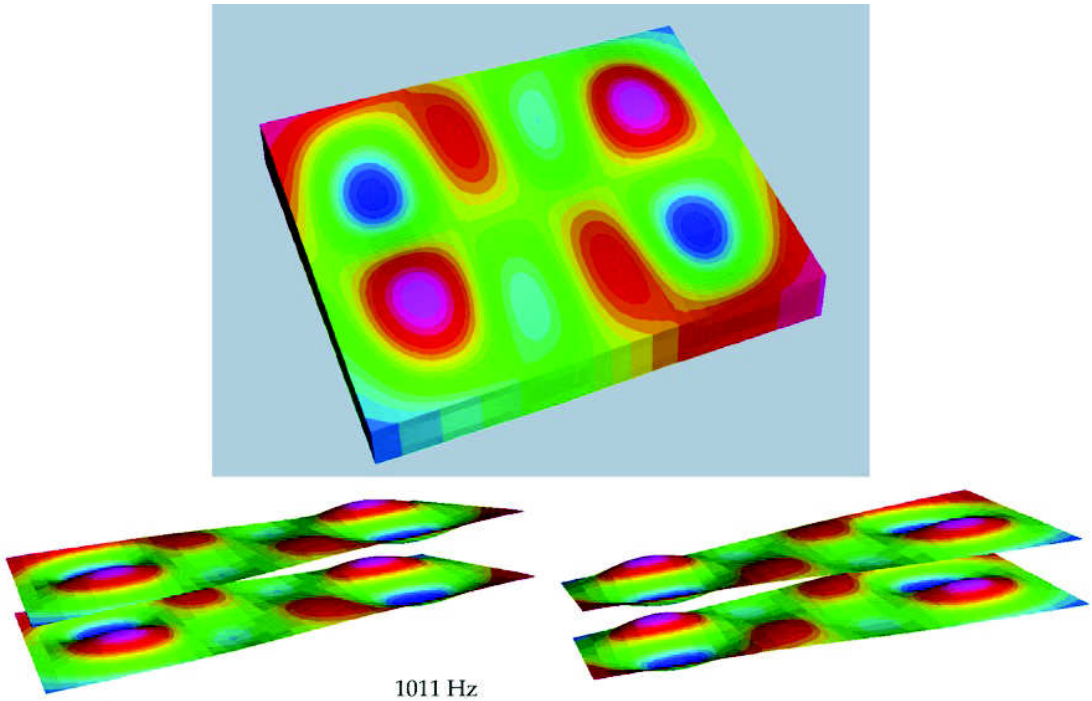

Figure 20: Contours of z displacement from two views onto the antisymmetric box mode at 1011 Hz. The lower panel shows the extremes of motion, emphasising the twist. Red = max. up, blue = max. down.

5 Normal modes under variations in box design

5.1 Unequal plate thicknesses

The effect on resonant frequencies of changing the thickness of the back plate, according to the Strand7 2D shell-plate model, is presented in Table 8 for thicknesses from $2 \cdot 5$ to 5 mm. Consistent with the theory given in previous articles on this web site, the frequency of each mode increases with thickness. For this box the average rate is 9% increase per millimetre relative to the frequency at $3{\cdot}65$ mm. In all cases mode 1 is the 'breathing' mode. Though each resonance is a property of the box as a whole, the two plates in general contribute differently. They have different displacement patterns and in some modes one plate may be almost undeformed. There is a tendency for the thinner plate to have the largest displacements, something which intuitively we might expect. An example of this is shown in side views of the second mode in Figure 21. This picture also shows the weak springs on which the box is supported.

One feature of Table 8 worth investigating is the pairs of modes in each column which have almost exactly the same frequency. To pick out the closeness of adjacent modes let us introduce the

mode	thickness of back plate (mm)						
number	$2 \cdot 5$	$3 \cdot 0$	$3 \cdot 5$	$3 \cdot 65$	$4 \cdot 0$	$4 \cdot 5$	$5 \cdot 0$
1	157	167	175	177	182	187	192
2	208	228	243	247	253	260	264
3	242	251	260	263	270	280	291
4	295	304	315	320	332	351	373
5	316	354	382	388	400	411	418
6	428	438	455	461	478	507	508
7	428	477	495	498	503	507	530
8	442	477	513	518	525	529	537
9	464	533	550	558	582	614	627
10	517	534	587	598	614	623	639
11	536	558	589	599	621	646	664
12	557	618	653	662	686	700	713
13	608	638	670	675	692	719	724
14	631	648	678	691	708	744	798
15	639	715	744	754	788	813	830
16	710	730	765	775	792	850	914
17	723	786	836	850	882	923	939
18	776	798	854	870	899	924	962
19	819	926	959	968	989	1023	1048
20	848	937	989	999	1016	1033	1065
21	905	952	998	1011	1047	1103	1104
22	914	963	1007	1022	1062	1111	1176
23	916	966	1057	1081	1099	1126	1183
24	931	1051	1115	1126	1186	1215	1215

Table 8: Resonant frequencies for a birch 3-ply rectangular box 300×250 mm for various thicknesses of back plate, the top plate's being fixed at $3 \cdot 65$ mm.

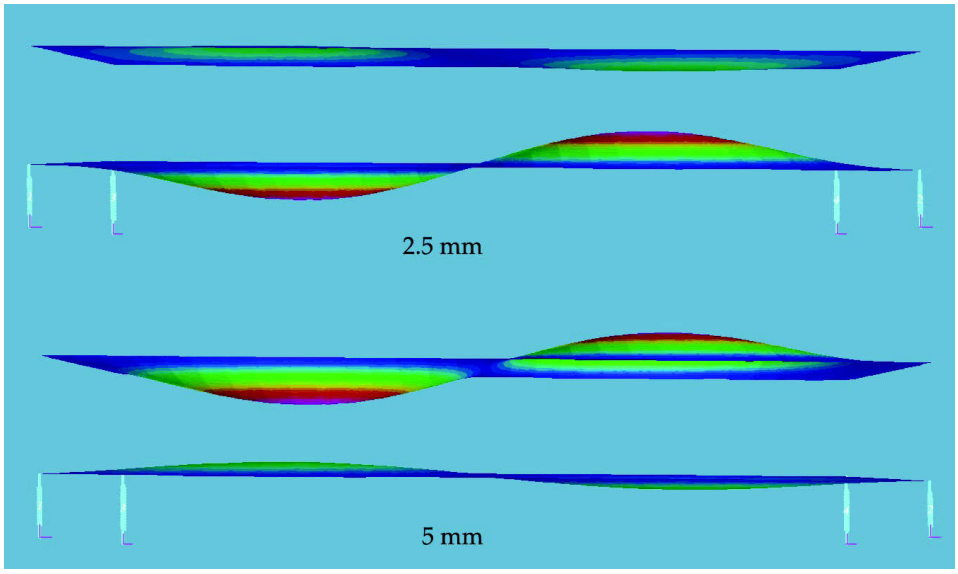

Figure 21: Side views of the box (ribs invisible) showing Mode 2 when the thickness of the back plate (lower of each pair) is $2 \cdot 5$ and $5 \cdot 0$ mm.

following statistic

$$P(k) \;=\; \frac{1}{\frac{f_{k+1}}{f_k} - 1} \;=\; \frac{f_k}{f_{k+1} - f_k} \tag{9}$$

where f_k is the frequency of the k^{th} mode. $P \to \infty$ as $f_{k+1} \to \; f_k$. Values of P are listed in Table 9, which matches Table 8. The lowest five pairs of modes have much the same wide spacing in pitch.

Figure 22 shows the z displacement of the two plates for modes 6 and 7 with back plate $2 \cdot 5$ mm thick. The bottom plate has almost the same displacement in each mode, whilst the top plate has a phase inversion. Otherwise they are very similar. In practice they would behave as a single mode. However, with the top plate capable of resonating in either sense, the mode excited in practice would depend critically on where the driving force was positioned.

The relation between the two adjacent modes in Figure 23 is different. These are modes 12 and 13 when the back plate is 4 mm thick. Both are antisymmetric, the top and back plates undergoing almost exactly the same motion in (x, y, z). Mode 12 is type (2-1), mode 13 is (3-1). They are genuinely different, but either could be excited depending on exactly how the box was driven.

I have not examined other adjacent pairs. Assuming that such mode overlapping is undesirable from the point of view of the violin maker, we would ideally want the values of P in any column of Table 9 to be all about equal and less than about 50. If the numbers > 100 are eliminated, the average of the others is about 24 for all thicknesses of back. This corresponds to about 4% difference in pitch, less than one semitone. In the search for evenly pitched resonances there is not a lot to choose amongst the seven thicknesses of back plate, though those at $2 \cdot 5$, $3 \cdot 5$ and $4 \cdot 5$ are marginally better and that at $3 \cdot 0$ mm the worst.

In summary, on the basis of this limited simulation, only a modest improvement towards spacing the resonances equally in pitch can be obtained by changing the thickness of one plate. It

seems likely that at least one pair of closely adjacent modes will occur, and the dynamic response at this frequency may be difficult to control.

mode	$P(k)$						
k	$2\cdot5$	$3\cdot0$	$3\cdot5$	$3\cdot65$	$4\cdot0$	$4\cdot5$	$5\cdot0$
1	3	3	3	3	3	3	3
2	6	10	15	15	16	13	10
3	5	5	5	5	4	4	4
4	14	6	5	5	5	6	8
5	3	4	5	5	5	4	5
6	**7928**	12	11	13	20	**1820**	23
7	32	**1619**	28	24	23	23	82
8	20	9	14	13	9	6	6
9	9	**290**	15	14	18	68	52
10	29	22	**243**	**561**	87	27	26
11	25	9	9	9	10	12	13
12	11	31	40	52	**114**	37	65
13	26	65	85	43	41	28	10
14	87	10	10	11	9	11	24
15	9	50	36	36	**173**	22	10
16	56	13	11	10	9	12	36
17	14	64	47	43	54	**1006**	42
18	18	6	8	9	10	9	11
19	28	78	32	31	36	**101**	64
20	15	63	**106**	80	33	15	27
21	**103**	90	**119**	98	69	**139**	15
22	**639**	**316**	20	17	29	72	**178**
23	59	11	18	24	13	13	37

Table 9: $P(k)$, a measure the closeness of adjacent resonant frequencies. Large values mean that adjacent resonances are very close together. Values $P > 100$ are shown in bold.

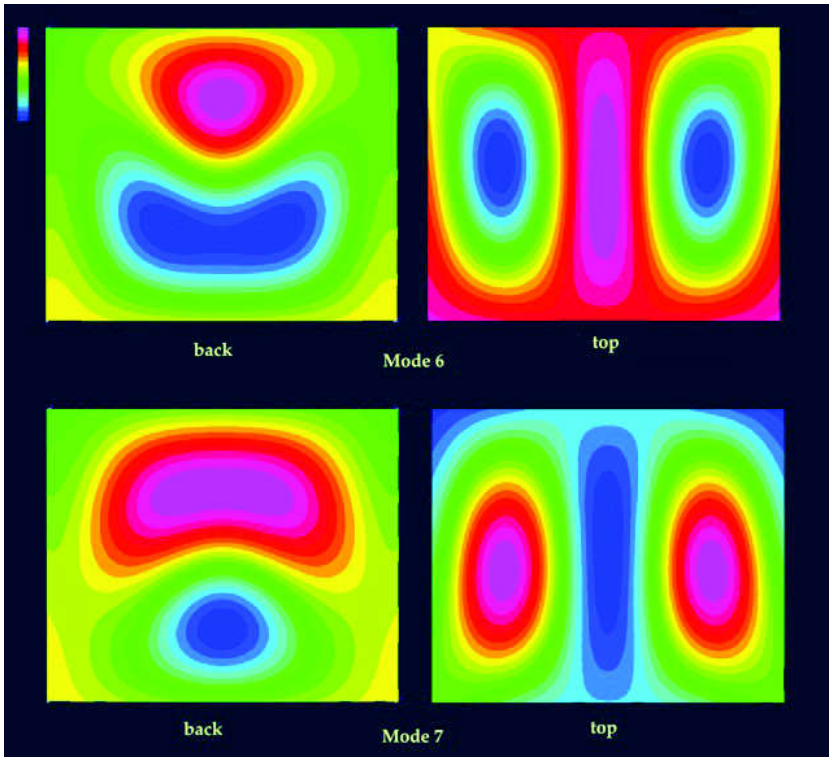

Figure 22: Contours of z displacement for two overlapping modes, 6 and 7, with back plate $2 \cdot 5$ mm thick. $P = 7928$. Red = max up, blue = max. down, green = node line.

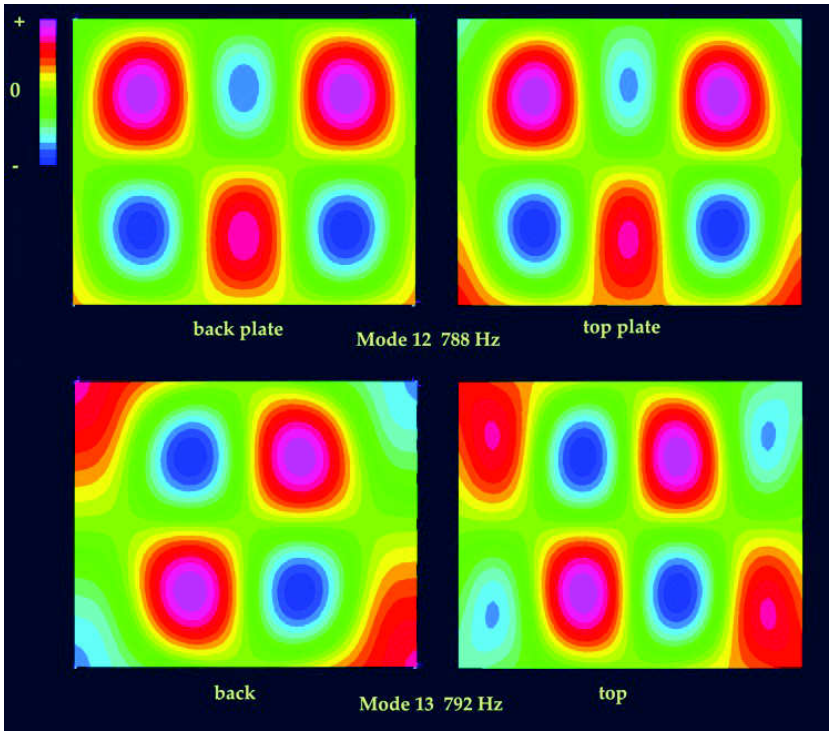

Figure 23: Contours of z displacement for two close modes, with back plate $4 \cdot 0$ mm thick.

5.2 Different plywoods

In my studies I have used three actual types of 3-plywood:

- all-birch, $3 \cdot 65$ mm thick,
- Far Eastern ply, $3 \cdot 60$ mm thick,
- a pink-red hardwood-faced ply, $2 \cdot 91$ mm thick.

In a previous article I described how I determined a set of elastic constants for all three types. Here FEA is used to predict the resonances of six boxes made with combinations of these materials for top and back plates. There is a concomitant difference in thickness with the pink hardwood ply, but I have accepted this rather than set the thickness to be $3 \cdot 65$ mm because with plywood one must accept the thickness as it is – any thinning would change the relative ply thicknesses and hence the orthotropic elastic constants.

The results for the six virtual boxes are listed in Table 10. We again see pairs of closely adjacent frequencies. As an example Figure 24 shows the modes at 258 and 261 Hz for a top of

top :	birch	birch	Far East	pink	pink	birch	birch
back:	birch	Far East	Far East	Far East	pink	pink	birch
	177	169	163	158	154	162	177
	247	**258**	258	247	233	**251**	247
	263	**261**	274	262	255	**252**	263
	320	341	357	343	322	321	320
	388	414	456	420	405	408	388
	461	472	479	454	442	424	461
	498	492	492	472	**461**	**468**	498
	518	507	**504**	494	**471**	**478**	518
	558	546	**512**	**502**	**473**	**549**	558
	598	569	533	**512**	**481**	**549**	**598**
	599	626	695	641	620	623	**599**
	662	692	748	721	680	643	662
	675	700	757	**729**	**706**	684	675
	691	760	771	**734**	**713**	**731**	691
	754	**785**	785	777	738	**738**	754
	775	**786**	811	791	778	777	775
	850	898	931	859	810	853	850
	870	**940**	**952**	**894**	**853**	885	870
	968	**947**	**955**	**896**	**863**	897	968
	999	978	992	946	916	**933**	**999**
	1011	1016	1012	**991**	935	**943**	**1011**
	1022	1055	1082	**997**	976	**995**	**1022**
	1081	1099	1093	1049	**994**	1003	1081
	1126	1106	1118	1073	**995**	1068	1126

Table 10: Strand7 predictions of resonant frequencies of boxes, 300×250 mm, with top and back plates of different plywoods. Grain is parallel to the shorter sides. Ribs $1 \cdot 72$ mm thick, 40 mm deep. Close resonances are shown in bold.

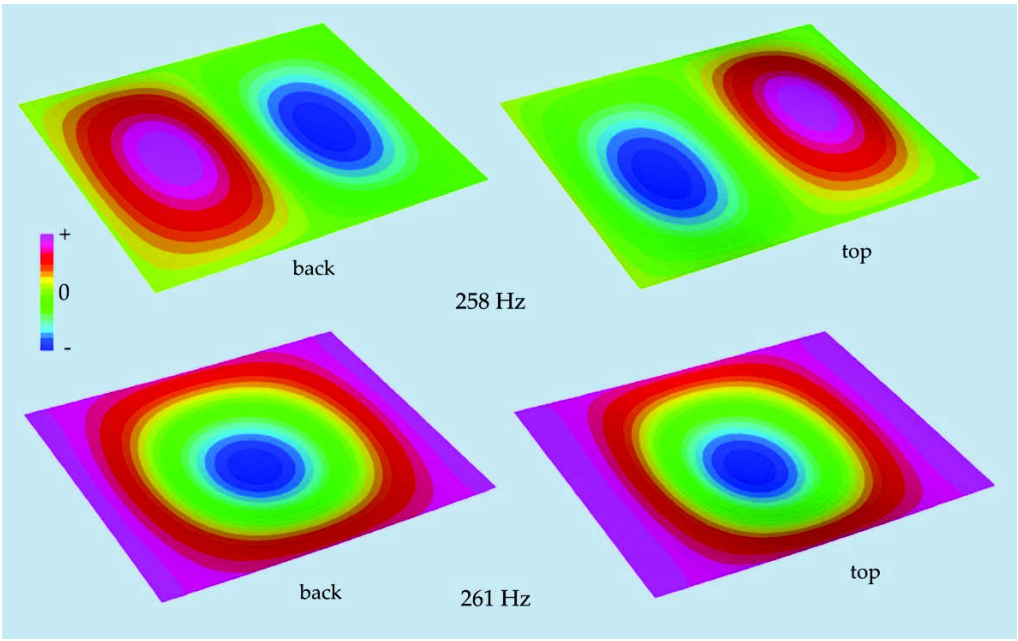

Figure 24: Two independent modes occurring at almost the same frequency in a rectangular box, top of birch ply, back of Far Eastern ply. Contours of z displacement; green = zero.

birch, back of Far Eastern ply. These are clearly quite different in character. To what extent this is specific to a rectangular shape, I cannot yet say. Moreover, these adjacent pairs would probably be quite different if the plate dimensions were different.

A violin is usually made with top plate of sitka spruce and back of curly maple. Slow grown spruce is used because of its resonant characteristic and harder surface. Being shaped from solid blocks, the violin maker can adjust the plates thicknesses in a way that cannot be done with plywood.

5.3 Changing the wood grain orientation

With an eye to violin making I have only considered changes in grain orientation which would maintain some static strength and resistance to static distortion. Therefore the back panel is kept with the grain orientation along the y axis whilst the top is made from either two or three panels of plywood glued together in a mirror symmetry design, Figure 25. The grain in the left and right panels is turned away from the y direction through an angle θ, making the misorientation of the two plates 2θ with respect to each other. Both plates are modelled as all-birch 3-ply, $3 \cdot 65$ mm thick.

Consider first the 2-panel design. The variation in modal frequencies with θ is graphed in Figure 26. At 90° the grain in the top plate is parallel to the long (x) axis. As seen in the previous two subsections, the lowest three modes are fairly resistant to change, and modes 2 and 3 do not separate very far in frequency. There is a persistent tendency for some or other pair of modes to have much the same frequency. Perhaps the separation of modes is greatest on average at about 35° and 70°. Figure 27 shows the z displacement contours of both plates for the first 8 modes of the 2-panel design with $\theta = 45°$. Although the back plate is partly obscured, we get some impression of the different motions of the two plates. The x axis in these pictures is into the page.

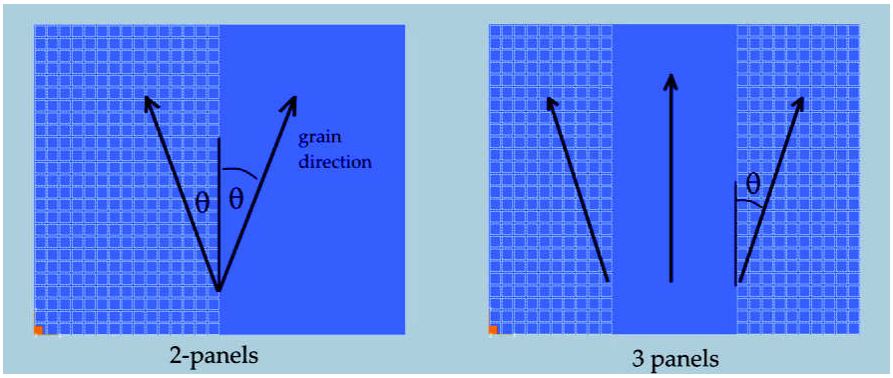

Figure 25: A top plate made from 2 or 3 panels of plywood with the surface grain running in the directions of the arrows, at angle θ to the y axis.

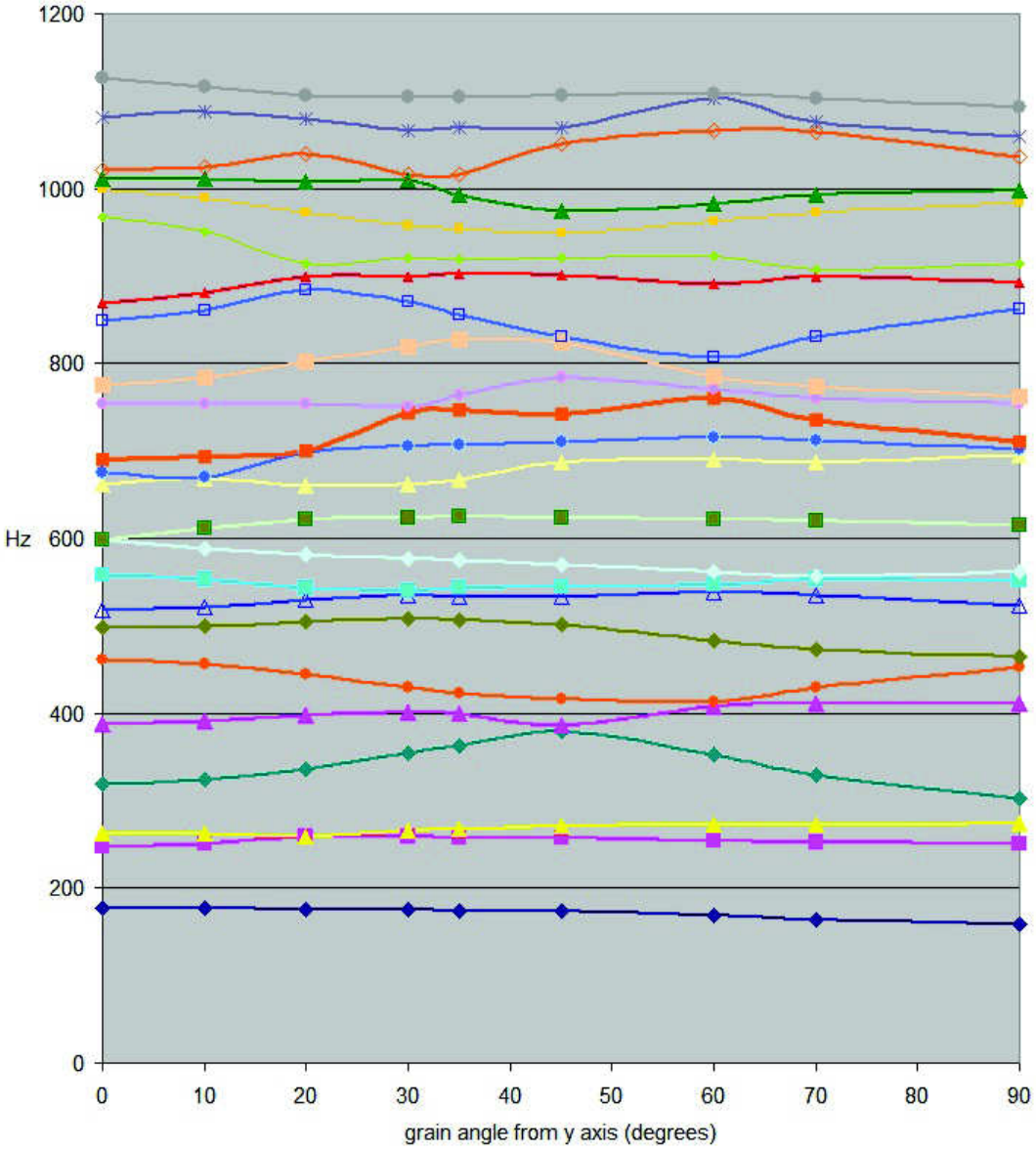

Figure 26: Variation of modal frequencies as the grain angle θ in the 2-panel top plate increases.

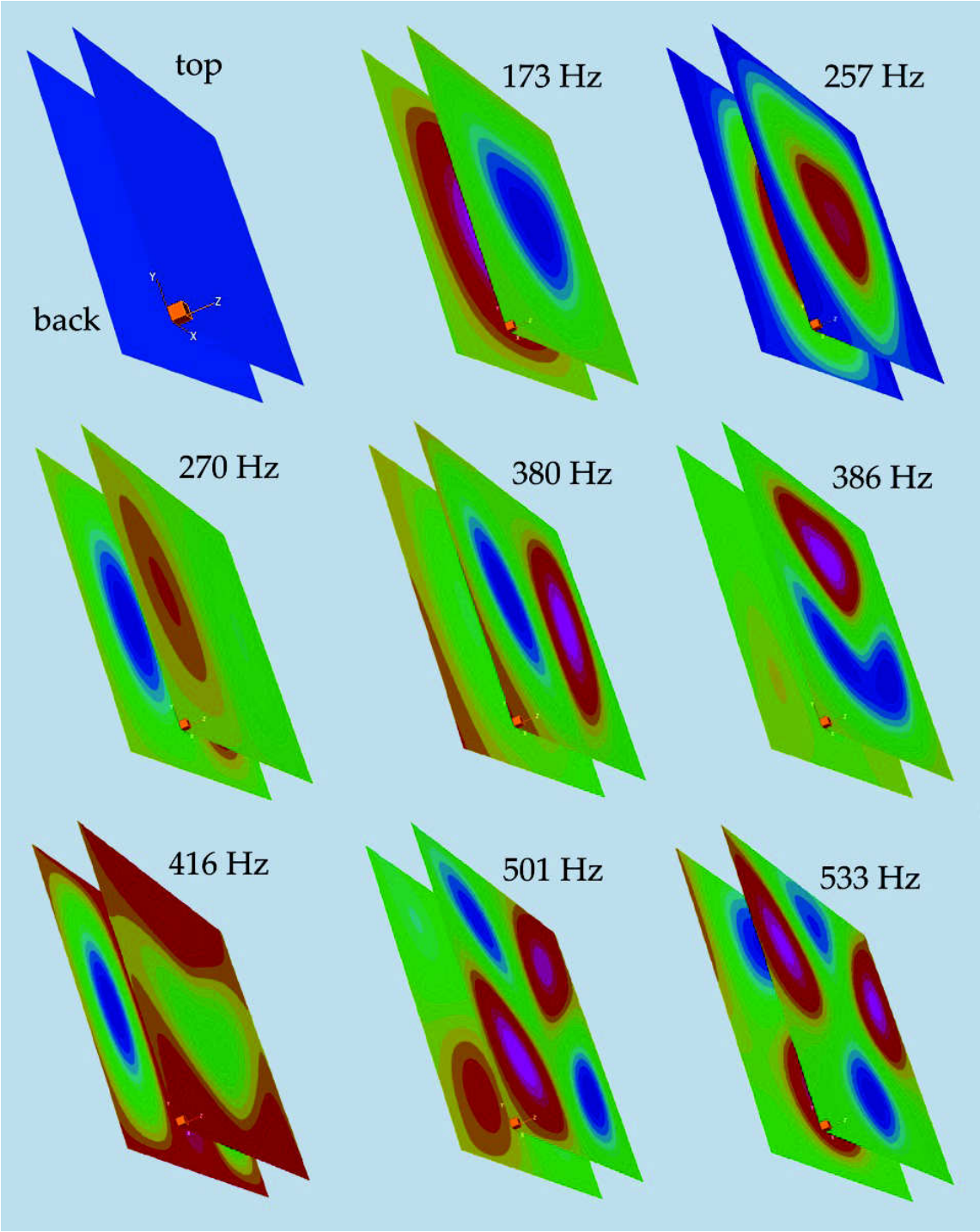

Figure 27: Oblique view of the top and back plates of box with 2-panel top plate. The z displacement contours of the first eight modes are shown. Red = max. up, blue = max. down, green = zero.

In the 3-panel design, Figure 25 right, in the central panel the grain is along the y axis. Table 11 lists the modal frequencies, with close pairs in bold type. It is striking how common it is to have a least one pair of overlapping modes.

0°	10°	20°	30°	40°	50°	60°	70°	80°	90°
177	177	178	179	179	178	176	173	171	170
247	249	253	258	**261**	**263**	**264**	**263**	**263**	**262**
263	263	263	264	**265**	**265**	**265**	**264**	**263**	**263**
320	321	325	330	336	340	341	342	342	342
388	392	400	408	413	417	419	421	421	422
461	462	466	472	479	**484**	**479**	470	464	462
498	499	500	498	494	**487**	**487**	485	482	480
518	520	525	532	**537**	**536**	534	534	535	536
558	556	550	544	**540**	**542**	544	**547**	**551**	**552**
598	586	576	570	566	563	559	**556**	**553**	**552**
599	610	617	620	621	621	621	621	621	621
662	**667**	663	662	669	685	703	714	718	719
675	**670**	684	**706**	711	716	723	734	746	751
691	694	700	**707**	727	**745**	755	**762**	**765**	**765**
754	754	754	752	751	**751**	758	**763**	**768**	**770**
775	779	789	801	809	810	802	791	780	**776**
850	855	868	878	884	889	897	879	864	859
870	877	895	915	927	**923**	902	905	**911**	**911**
968	962	953	947	**943**	**930**	922	917	**915**	**917**
999	**990**	974	958	**947**	950	949	949	950	950
1011	**1009**	1001	994	**991**	965	961	964	967	968
1022	**1029**	1046	1028	**995**	1009	1029	1047	1059	1063
1081	1084	1080	1099	**1105**	1088	1081	1091	**1106**	**1106**
1126	1117	1105	1114	**1110**	1106	1107	1107	**1106**	**1112**

Table 11: The 3-panel design of top plate, listing the modal frequencies as the grain angle θ increases away from the y direction in the two side panels.

5.4 Stitch-glued lengths of edge

Figure 28 shows in yellow six sections of edge along which the top plate is not fastened to the ribs. Table 12 lists the modal frequencies of this box when the numbers of unglued sections increases from none, then Section 1 only, then Sections 1, 2 and 3 along the long sides, and finally all six sections. In this last stage of ungluing one corner is completely free. Note how the modal frequencies decrease as the constraints are removed. The displacements in two modes with all six sections unglued are shown in Figures 29 and 30.

I have not heard of ungluing sections of edge being used as a means of adjusting the resonances of a violin belly, but it might have possibilities. It would be necessary to remove some of the rib locally to prevent a buzzing noise due to the plate rubbing against the rib when played.

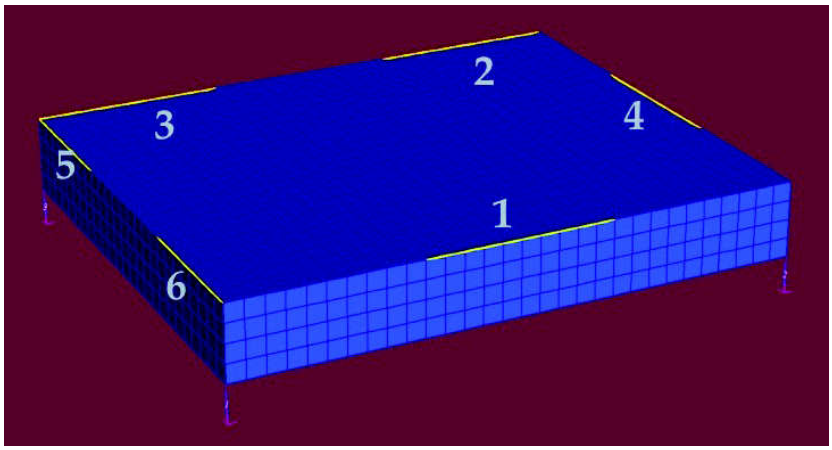

Figure 28: A rectangular box where the top plate is unglued along the six yellow sections of edge.

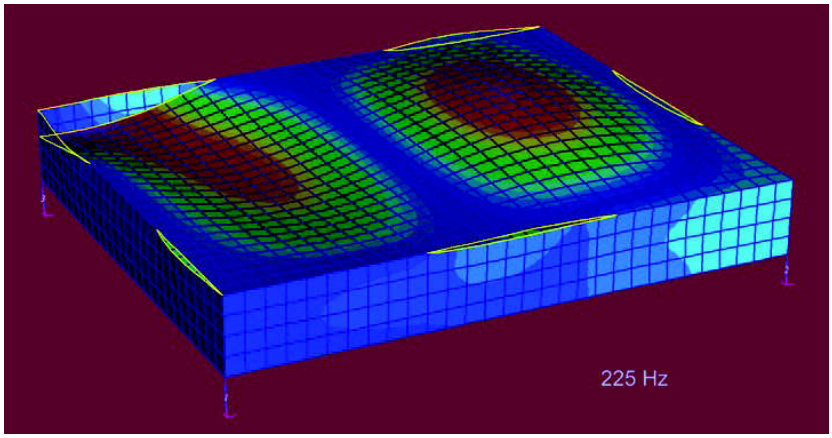

Figure 29: Contours of displacement magnitude of box at 225 Hz. Green = zero.

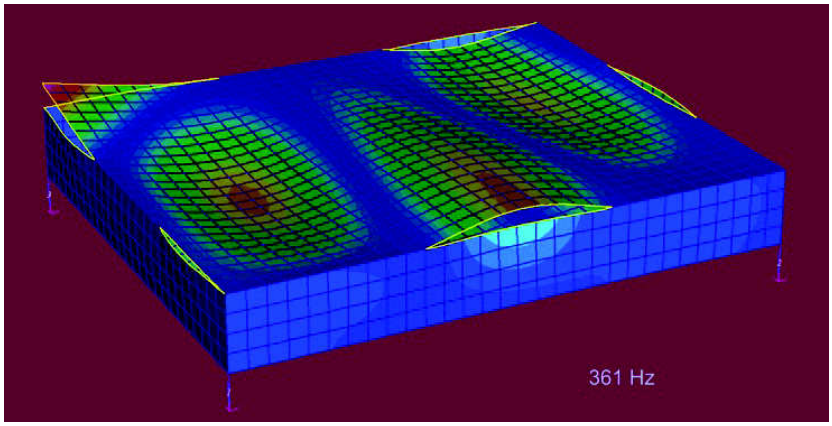

Figure 30: Displacement contours of box with partially unglued edges at 361 Hz.

unglued section numbers				
none	1	1, 2, 3	1, 2, 3, 4	all six
177	167	164	163	162
247	**243**	**237**	232	225
263	**246**	**239**	239	235
320	316	305	300	**294**
388	380	369	360	**298**
461	428	**422**	**419**	361
498	470	**424**	**420**	415
518	488	451	444	434
558	534	497	494	459
598	**593**	**544**	543	529
599	**598**	**551**	550	539
662	639	596	578	556
675	660	651	628	573
691	679	654	652	610
754	722	**702**	699	647
775	762	**704**	703	685
850	831	737	732	713
870	840	765	760	739
968	870	**856**	804	765
999	889	**861**	853	774
1011	983	**868**	866	794
1022	1000	905	875	826
1081	1004	933	916	856
1126	1045	961	930	859

Table 12: 'Stitched edges'. Modal frequencies (Hz) of rectangular box in which the top plate is unfixed along an increasing numbers of sections of edge. Section numbers refer to Figure 28. Closely spaced frequencies are marked in bold.

5.5 Unequal plate sizes

Changing the length or breadth of, say, the top plate may change not only its size but its aspect ratio, so the possible variations of size and shape, even for a rectangle, are many. Clearly, if the two plates are not the same size, the ribs will no longer be at right angles to the plates. The calculations here maintain one plate at 300×250 mm. I evaluated the normal modes for variation in the x and y side lengths of the other plate by about $\pm 6 \cdot 6\%$. Counting also the reference size of 300×250 mm, this gives nine length combinations in all. Figure 31 shows the Strand7 model for one such. The grain direction in both plates in the y direction is always parallel to the shorter side. Again all-birch ply $3 \cdot 65$ mm thick is modelled.

The results are presented in two ways. First, Table 13 lists the resonant frequencies in order, taking the combinations of plate dimensions in four sets, each with variation either side of the central value. For instance, the first panel has the x side length varying whilst the y length remains at 250 mm.

The second presentation is in Figure 32. Here the six surface graphs and associated array of frequencies relate to the lowest six modes respectively. The top left panel is annotated above and the other panels follow suit. The red dots at the intersections in the first graph show the nine values of frequency in the array above. Although all graphs show that the frequency is least for the largest plates, the dependence on x and y does vary with mode. In the 2nd, 4th and 6th modes the frequency is almost constant if x and y are scaled in opposite senses, so keeping the plate's area roughly constant. Note also how almost every column has at least one pair of closely adjacent frequencies.

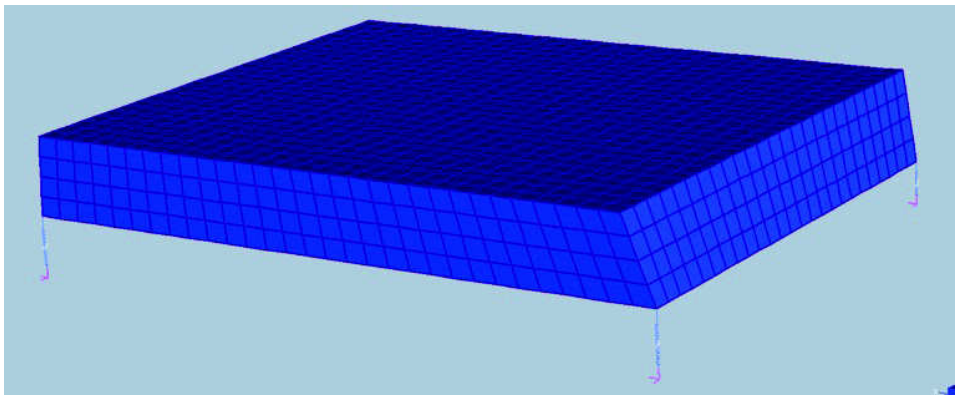

Figure 31: Mesh model of box with top plate 300×250 mm, back 320×234mm. Three of the supporting soft springs can be seen.

x mm	284	300	320	300	300	300	234	300	267	234	300	267
y mm	250	250	250	234	250	267	320	250	284	284	250	320
	179	177	176	185	177	167	184	177	169	187	177	165
	254	247	239	254	247	239	247	247	247	259	247	230
	267	263	258	274	263	252	270	263	256	278	263	247
	330	320	311	330	320	311	320	320	319	340	320	303
	403	388	368	394	388	383	376	388	399	407	388	360
	482	461	447	472	461	451	456	461	467	492	461	439
	507	498	486	511	498	474	501	498	485	517	498	461
	531	518	503	529	518	497	514	518	506	541	518	485
	559	558	**557**	591	558	527	565	558	533	592	558	524
	604	**598**	**558**	602	**598**	571	590	**598**	575	622	**598**	550
	620	**599**	595	635	**599**	593	628	**599**	618	643	**599**	569
	694	662	**640**	671	662	**654**	645	662	**673**	**708**	662	630
	702	675	**647**	690	675	**655**	662	675	**677**	**711**	675	**635**
	704	691	678	712	691	**658**	705	691	687	**719**	691	**636**
	772	754	740	**793**	754	734	772	754	743	801	754	712
	787	775	752	**798**	775	744	786	775	764	814	775	725
	880	850	815	873	850	828	820	850	852	**912**	850	**810**
	913	870	829	881	870	866	853	870	908	**916**	870	**810**
	981	968	952	1005	968	933	984	968	947	1016	968	915
	1020	999	961	1022	999	960	985	999	981	1042	999	926
	1039	1011	978	1030	1011	980	992	1011	1003	1069	1011	955
	1079	1022	984	1044	1022	1004	1016	1022	1046	1081	1022	965
	1101	1081	1018	1095	1081	1053	1059	1081	1094	1104	1081	981
	1161	1126	1105	1157	1126	1087	1110	1126	1096	1224	1126	1085

Table 13: Modal frequencies in Hz as the x (left panel) or y (second panel) side lengths of one plate of rectangular box are varied by about 6%. Third and fourth panels have both x and y varying. Bold face highlights closely spaced modes.

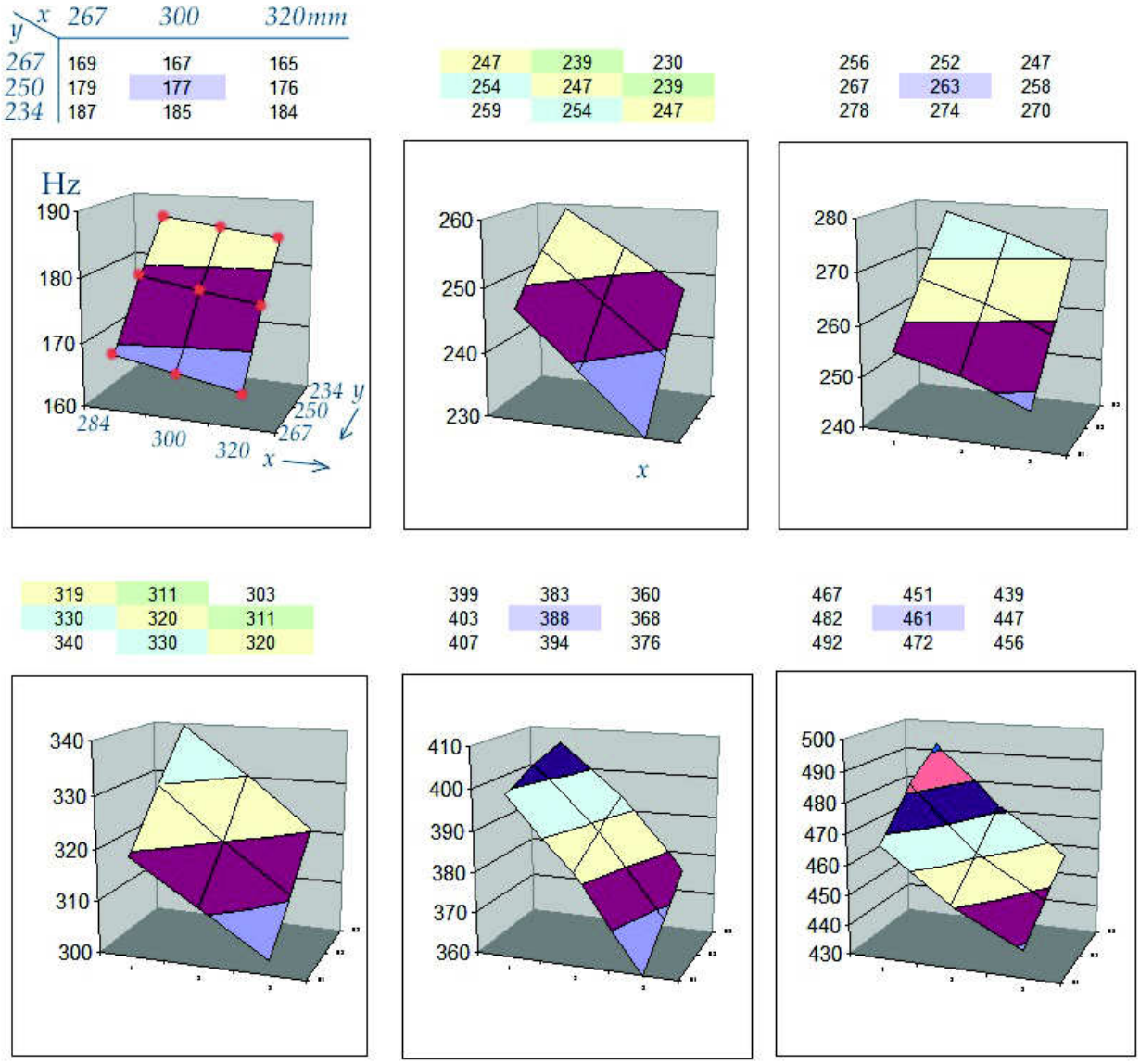

Figure 32: Variation in resonant frequency of the six lowest modes of a rectangular box as the side lengths of one plate are changed from a central value of 300 mm in x, 250 mm in y. The other plate is maintained at this central size.

6 Conclusion

This article has moved from the vibrational modes of a single plywood rectangle to the modes of a cuboidal box. I have present comparisons with experiment for a single plate glued onto a base (Figure 2) and a closed plywood box (§4.2). Relying on the modelling capabilities of Strand7, we have looked at the effect of the boundary conditions which describe how the plate is glued to its support. We have also amassed a sizeable database on the changes in resonance due to small changes in the construction of the box – changes in plate thickness, wood type, grain orientation, edge gluing and plate size.

	Mode	lowest	2nd	10th	20th	24th	30th
free	f (Hz)	54	70	434	949	1270	1538
plate	$f/54$	1	1·3	8·0	17·6	23·5	28·5
	$f/70$		1	6·2	13·6	18·1	22·0
SS	f (Hz)	144	204	1032	1761	2002	2476
plate	$f/144$	1	1·4	7·2	12·2	13·9	17·2
	$f/204$		1	5·1	8·6	9·8	12·1
fixed	f (Hz)	306	367	1297	2089	2342	2779
plate	$f/306$	1	1·2	4·2	6·8	7·7	9·1
	$f/367$		1	3·5	5·7	6·4	7·6
box	f (Hz)	177	247	598	999	1126	
equal plates	$f/177$	1	1·4	3·4	5·6	6·4	
	$f/247$		1·0	2·4	4·0	4·6	

Table 14: The density of modes over frequency. Frequencies, and pitch ratios, at which selected modes occur for four structures involving one or two rectangular plates of all-birch 3-ply, 300×250 mm, $3 \cdot 65$ mm thick.

In almost all situations at least two modes have almost the same frequency. This is largely due to the density of modes over frequency being much higher in a box structure than for a single free plate. Table 14 draws together results from previous sections to show that the first 24 modes of a free plate are spread over a frequency ratio of 23 (nearly 5 octaves), but the first 24 modes of a box are squeezed into a ratio of about 6 (less than 3 octaves). The tables and graphs show how varying one parameter or another can change the modal frequencies by fairly small amounts but in different senses so that modes which were close become separated while others which were separate are brought together. This must cast doubt of the scope for controlling modes to preselected frequencies. We have also seen the significant consequences of allowing a section of edge in a box structure to become unglued. So any box structure which became damaged or in which the glue cracked through age could suffer an uncontrolled change in resonant frequencies. These points may be important in violin making and maintenance.

Since the literature on violins makes much of tuning the plates, here is a summary of some of the ways this can be achieved. These steps increase the frequency:

- smaller plate area,
- smaller thickness,

- more highly constrained edges,
- less dense material,
- stiffer material.

Of course, such changes would affect the amplitude of vibration and hence the intensity of sound radiated, effects which I have not yet addressed. The next stages towards modelling a violin will include :

- considering the Helmholtz resonance of the air inside the box cavity,
- examining the dynamic response of a box structure to a prescribed periodic driving force applied through something resembling a violin bridge,
- modelling a box with flat plates but the shape of a violin,
- calculating sound tone and loudness of these boxes by modelling the acoustic radiation from them,
- modelling the domed plates, necessary to withstand the large static load applied through the bridge from the tension in the four strings.

These will be addressed in future papers on www.mathstudio.co.uk.

I am most grateful to the management of Strand7 for access to their program, and to the management of the LISA for use of an advance copy of LISA 8.

John Coffey, Christmas 2012, revised with new material (§4.1 and 4.2) February 2013